N/S/\

Technical Memorandum **82006**

Weather and Climate Needs for Lidar Observations from Space and Concepts for Their Realization

David Atlas and C. Laurence Korb

JUNE 1980

National Aeronautics and
Space Administration

Goddard Space Flight Center
Greenbelt, Maryland 20771

UTTL: Weather and climate needs for Lidar observations from space and concepts
      for their realization --- wind, temperature, moisture, and pressure data
      needs
AUTH: A/ATLAS, D.; B/KORB, C. L.
CORP: National Aeronautics and Space Administration. Goddard Space Flight
      Center, Greenbelt, Md.   AVAIL.NTIS
SAP: HC A04/MF A01
COI: UNITED STATES Submitted for publication   Presented at the OSA Conf. on
      Coherent Laser Radar for Atmospheric Sensing, Aspen, Colo., 15-17 Jul.
      1980
MAJS: /*ATMOSPHERIC PRESSURE/*CLOUD PHOTOGRAPHY/*HUMIDITY/*RADAR IMAGERY/*
      TEMPERATURE PROFILES/*WEATHER FORECASTING/*WIND MEASUREMENT
MINS: / BACKSCATTERING/ LATENT HEAT/ OPTICAL RADAR/ PATTERN RECOGNITION/
      SATELLITE-BORNE RADAR
ABA: J.M.S.

ENTER:

WEATHER AND CLIMATE NEEDS FOR LIDAR OBSERVATIONS FROM SPACE AND CONCEPTS FOR THEIR REALIZATION*

David Atlas
Laboratory for Atmospheric Sciences

and

C. Laurence Korb
Earth Observations Systems Division

June 1980

NASA/GODDARD SPACE FLIGHT CENTER
GREENBELT, MARYLAND

N80-33057 #

WEATHER AND CLIMATE NEEDS FOR LIDAR OBSERVATIONS FROM SPACE AND CONCEPTS FOR THEIR REALIZATION

by

David Atlas[1]

C. Laurence Korb[2]

ABSTRACT

The spectrum of weather and climate needs for Lidar observations from space is discussed. This paper focuses mainly on the requirements for winds, temperature, moisture, and pressure. Special emphasis is given to the needs for wind observations and it is shown that winds are required to realistically depict all atmospheric scales in the tropics and the smaller scales at higher latitudes, where both temperature and wind profiles are necessary. The need for means to estimate air–sea exchanges of sensible and latent heat also is noted. A concept for achieving this through a combination of Lidar cloud top heights and IR cloud top temperatures of cloud streets formed during cold air outbreaks over the warmer ocean is outlined. Recent theoretical feasibility studies concerning the profiling of temperature, pressure, and humidity by differential absorption Lidar (DIAL) from space and expected accuracies are reviewed. Initial ground based trials provide support for these approaches and also indicate their direct applicability to path–average temperature measurements near the surface. An alternative approach to Doppler Lidar wind measurements also is presented. The concept involves the measurement of the displacement of the aerosol backscatter pattern, at constant height, between two successive scans of the same area, one ahead of the space-craft and the other behind it, a few minutes later. Finally, an integrated space Lidar system capable of measuring temperature, pressure, humidity, and winds which combines the DIAL methods with the aerosol pattern displacement concept is described briefly.

---

[1]Laboratory for Atmospheric Sciences
[2]Earth Observations Systems Division, NASA/Goddard Space Flight Center, Greenbelt, MD 20771.

CONTENTS

TABLES

ILLUSTRATIONS

WEATHER AND CLIMATE NEEDS FOR LIDAR OBSERVATIONS FROM SPACE AND CONCEPTS FOR THEIR REALIZATION

1. INTRODUCTION

The needs for and potential applications of lidar observations to research and operations in the environment are so broad that it is impossible to cover them in a single paper. Therefore, this paper will focus mainly on those in the general arena known as "weather and climate." These are not necessarily the most important problems which need attention within the broader realm of the environmental sciences, but are a representative subset.

A few caveats are in order:

(1) While the focus will be on space-based observing systems, it is recognized that there are a host of significant lidar studies and applications which are better done either from the ground, aircraft, or balloons. Also, that measurements from space will frequently have to be supported by such ancillary observing systems, and that the logical development cycle will almost always involve a progression from ground to aircraft to space-based experiments.

(2) Although this paper is focused mainly on lidar, the needs for other systems will be considered also since it is clear that a combination of other sensors will be required. Indeed, we will show how lidar can be combined with other remote sensors to provide hybrid measurement capabilities.

The programs of recent conferences and reviews in the literature give a sense of the exceedingly broad range of potential applications of lidar to the atmospheric sciences, ranging from the lowermost levels of the troposphere to the outer reaches of the magnetosphere. NASA has conducted an in-depth survey of the scientific problems and the feasibility of conducting meaningful lidar experiments from the space shuttle. The interested reader is referred to the report "Shuttle Atmospheric Lidar Research Program" (NASA, 1979). While there is overlap between

1

the latter report and what is discussed here, our discussion will be restricted mainly to weather and climate problems in the troposphere and stratosphere with some elaboration on a few key problem areas such as winds and air–sea interactions. Another NASA survey report deals with the entire realm of tropospheric air quality and discusses requirements for lidar measurements of tropospheric trace gases and aerosols (NASA, 1980a).

2. WEATHER AND CLIMATE – GENERAL

Weather prediction on both the global and regional scales remains the dominant scientific and operational problem facing the meteorological community. Recently, the concerns with the societal impacts of climate variability on the shorter time scales (i.e., months to years) and climatic change over decades has greatly heightened the activity in climate research, with much of the focus aimed at the question of climate predictability.

By and large, the approach to both numerical weather prediction and climate prediction proceeds by the same general route; namely, through the use of General Circulation Models (GCM's) and high speed computers. The differences between the two approaches are mainly that: (1) in global weather prediction the concern is with the detailed specification of the weather on regional scales of the order of 1000 km around the globe and time scales of up to 10 days, while climate prediction aims at the statistical description (i.e., mean, variance) of the weather over a month or more over larger regions; and (2) in the case of climate, there is also a need to observe those forcing parameters which have longer time constants and are thought to give the climate some long term "memory"; by and large, these are mainly surface properties such as sea surface temperature, snow and sea ice, albedo, and soil moisture, and the more slowly varying radiatively active gases and aerosols.

These two basic differences in approach to weather and climate also have important implications for the observing systems in terms of accuracy, precision, and time/space resolution. Because climate deals with time/space averaging, sampling rates can generally be reduced; by the same token,

2

precision and accuracy must be increased simply because the climate perturbations are averaged down ensembles of the weather fluctuations. However, where the "weather" measurement systems are characterized by random errors, the required climatic accuracy often can be obtained simply by averaging a large observational set. It is in this regard that all the basic measurements required for numerical weather prediction may also be used for climatic purposes. However, the long time scales of interest put a high premium on instrument stability and intercalibration, and additionally, on the uniformity and accessibility of the operational weather data.

Since both weather and climate prediction begin with the basic hydrodynamic and thermo-dynamic equations and aim at predicting the future state of the environment from the present one, both are initial value problems which depend critically on the accurate specification of the state at time zero. Presuming that the models incorporate all the relevant physics and that the numerical computational schemes are accurate, future progress depends in large part upon the improved qual-ity and quantity of observations. This view is generally shared by the numerical prediction community, which has made remarkable progress in model development, but require better ob-servations to initialize and test their models and diagnose their deficiencies. Indeed, this was one of the primary motivations of the year long Global Weather Experiment (GWE) completed in December 1979. Another perspective on this subject recently was presented by McPherson,[1] and Kreitzberg[1] deals with corresponding requirements for short range local and regional predictions.

3. OBSERVATIONAL REQUIREMENTS

A comprehensive list of observational requirements for the diagnosis and modeling of climate on seasonal and interannual time scales is given in Table 1 (NASA, 1977). Requirements for studies of the climate on decadal and longer time scales have been omitted, mainly for reasons of brevity, although it should be noted that such problems involve measurements and monitoring of long term

---

[1]Presentations at the Optical Society of America Conference on Coherent Laser Radar for Atmospheric Sensing, Aspen, Colorado, July 15-17, 1980.

Table 1

Observational Requirements for Climate on Monthly, Seasonal, and
Interannual Time Scales

	Parameter	Desired Accuracy	Base Requirement	Horizontal Resolution	Vertical Resolution	Temporal Resolution	Lidar Capability
Weather Variables (•Basic FGGE Meas.)	• Temp. Profile	1°C	2°C	500 km	200 mb	12-24 Hrs.	B
	• Surface Pres.	1 mb	3 mb	500 km	—	12-24 Hrs.	B
	• Wind Velocity	3 m/sec	3 m/sec	500 km	200 mb	12-24 Hrs.	C
	• Sea Sfc. Temp.	0.2°C	1°C	500 km	—	3 Days	B/S
	• Humidity	7%	30%	500 km	400 mb	12-24 Hrs.	B
	Precipitation	10%	25%	500 km	—	12-24 Hrs.	NA
	Clouds			100 km	—	1 Day	
	a. cloud cover	5%	20%				B
	b. cloud top temp.	2°C	4°C				} B/S
	c. albedo	0.02	0.04				
	d. total liq. H_2O Content	10 mg/cm²	1.50 mg/cm²				
Ocean Parameters	Sea Sfc. Temp.	0.2°C	1°C	500 km	—	1 Month	B/S
	Evaporation	10%	25%	500 km	—	1 Month	} NA
	Sfc. Sens. Heat Flux —	10 W/m²	25 W/m²	500 km	—	1 Month	
	Wind Stress	0.1 Dyne/cm²	0.3 Dynes/cm²	500 km	—	1 Month	
Radiation Budget	Clouds (Effect on Radiation)			500 km		1 Month	
	a. cloud cover	5%	20%				B
	b. cloud top temp.	2°C	4°C				} B/S
	c. albedo	0.02	0.04				
	d. total liq. H_2O Content	10 mg/cm²	50 mg/cm²				
	Regional Net Rad. Components	10 W/m²	25 W/m²	500 km	—	1 Month	
	Eq.-Pole Grad.	2 W/m²	4 W/m²	1000 km Zones		1 Month	} B/S
	Sfc. Albedo	0.02	0.04	50 km	—	1 Month	
	Sfc. Rad. Budget	10 W/m²	25 W/m²	500 km	—	1 Month	
	Solar Constant	1.5 W/m²	1.5 W/m²	—	—	1 Day	} NA
	Solar UV Flux	10% per 50 Å Interval	—	—		1 Day	

Land, Hydrology, Vegetation

Precip., Sfc. Albedo, Soil Moisture (Sfc., Root zone) Vegetation Cover, Evapotranspiration, Plant Water Stress

Cryosphere

Sea Ice (% open water), Snow Cover, Snow Water Content

4

trends in radiatively active trace gases and aerosols to which lidar also is applicable. The first subset of parameters labeled "weather variables" includes the requirements for global weather. Table 2 provides a corresponding list of requirements specified for the first GARP Global Experiment (FGGE), now called the Global Weather Experiment (GWE) (WMO–ICSU, 1973). By and large, the latter agree closely with the climate requirements in Table 1, except for the case of winds; these are specified at $2\,m\,sec^{-1}$ for GWE and $3\,m\,sec^{-1}$ for climate. Also, Table 2 shows preliminary results obtained as a result of the initial analyses of the early data from the GWE. These are discussed further below.

It is not possible to review in this report the rationale by which these observational requirements were established; instead, reference may be made to the appropriate documents which discuss them at length (NASA, 1977; NASA, 1974, WMO–ICSU, 1973).

We have reviewed the listing in Table 1 and provided a subjective judgement as to whether or not the measurement requirement could be met or supported through the use of lidar. These assessments are shown in the last column according to the following code:

A — ready; feasibility studies completed and technology is available.

B — probably feasible; experiments need to be conducted and/or technology needs some development.

C — reasonable lidar concept available but full feasibility studies and experiments need to be conducted and/or major advances in technology are required.

In addition, the symbol S indicates where lidar is applicable in a supporting role, while NA signifies "not applicable." None of the present approaches are believed to fall into category A.

Before elaborating on specific parameters, some general remarks are in order. First, while much development is required, it seems likely that lidar will ultimately be capable of measuring all the basic state variables and winds within the base requirements for accuracy both for climate and global weather. It is also clearly applicable to the entire realm of cloud measurements, including

5

Table 2

Data Requirements for FGGE and Preliminary Results

BASIC PARAMETERS		HORIZONTAL RESOLUTION (km)	VERTICAL RESOLUTION		ACCURACY	FREQUENCY*	GLOBAL RMS FIT BETWEEN OBJECTIVE ANALYSIS AND OBSERVATION
			TROPOSPHERE	STRATOSPHERE			
MID AND HIGH LATITUDES	TEMP.	500	4 LEVELS	3 LEVELS	±1°K	1/DAY	±1.7°K SATELLITE
	WIND	500	4 LEVELS	3 LEVELS	±2m/SEC	1/DAY	**
	REL. HUMID	500	2 DEGREES OF FREEDOM		±30%	1/DAY	±10% RAWINSONDE
	SEA SFC. TEMP.	500			±1°K	3 DAY AVG.	±2°K AVHRR
	PRESSURE	500			±0.3%	1/DAY	±2MB SURFACE SHIPS
TROPICS	WIND	500	4 LEVELS	3 LEVELS	±2m/SEC	1/DAY	
	TEMP.	500	4 LEVELS	3 LEVELS	±1°K	1/DAY	
	REL. HUMID	500	2 DEGREES OF FREEDOM		±30%	1/DAY	
	SEA SFC. TEMP.	500			±1°K	3 DAY AVG.	

ADDITIONAL PARAMETERS:

- CLOUD, SNOW & ICE COVER
- PRECIPITATION AREA & INTENSITY
- SOIL MOISTURE
- EARTH RADIATION BUDGET
- SEA TEMPERATURE/CURRENTS

*2 PER DAY WOULD BE HIGHLY DESIRABLE FOR ALL PARAMETERS EXCEPT SEA SURFACE TEMPERATURE

** WINDS	MSEC⁻¹
RAWINSONDE	±4
AIRCRAFT	±9
ASDAR	±7
GEOSYNCHRONOUS SAT., NESS W.	±6
NAVAIDS (TROPICS)	±2.5
CONSTANT LEVEL BALLOONS (TROPICS)	±5
DROPWINDSONDE (TROPICS)	±3

cloud top height, cover, and cloud water phase. But it is equally or more important as an aid in support of other passive and active sensors, and it is in some of these realms that it is likely to be ready for near term application.

For example, in the case of cloud track winds obtained with geosynchronous satellite (GEOS), the cloud heights must be known to assign the winds to the proper level. Until stereo heights are available from pairs of GEOS, this can be done by lidar. By the same token, cloud heights are required in radiation budget studies because the net effects of clouds are exceedingly sensitive to their heights. Similarly, cloud heights aid in deducing cloud liquid water content (LWC) in two ways: through estimates of the LWC released adiabatically between deduced cloud base and cloud top, or by determining the depth of the cloud layer which is contributing to the radiative brightness (or attenuation) of microwave sensors sensitive to cloud water.

Although aerosol profiles are not explicitly listed in Table 1, they are of obvious importance in the radiation budget. They are also exceedingly important in many other ways. For example, corrections for aerosols and absorbing gases (especially CO_2 and H_2O) must be made in virtually every measurement of surface properties; sea surface temperature, one of the key climate variables, is a case in point. Unless IR measurements can be corrected for water vapor absorption and emission, it is unlikely that the base accuracy of $1°C$ will ever be obtained, let alone the desired accuracy of $0.2°C$. Lidar measurements of H_2O profiles by differential absorption lidar (DIAL) methods should provide the information to permit the necessary corrections. In addition, discontinuities in aerosol concentration mark both the tropopause and the height of the boundary layer; if these heights are known from lidar observations, the retrievals of temperature and moisture profiles by passive methods would be improved greatly by constraining them to fit the height measurements.

Measurements of the height of the boundary layer, either by scatter from aerosols or boundary layer clouds, would be of exceedingly great value throughout the atmospheric sciences. Such data

7

are required especially in those regional and global numerical models which carry the height of the planetary boundary layer (PBL) as a prognostic variable. Also, in the area of air–sea interactions, indicated in Table 1 by entries under evaporation, surface sensible heat flux and ocean wind stress, physical interpretation of the time/space variability of the boundary layer height can provide very good estimates of the heat and moisture fluxes. This will be elaborated on further below.

From this brief discussion, one can sense the wide variety of significant roles which space-based lidar will play in weather and climate in the years ahead. These general remarks will now be amplified in a few key problem areas.

4. WINDS

There is an increasingly large and persuasive body of studies demonstrating the need for and value of wind measurements in improving the accuracy of predictions on both the regional and global scales. The vast wind data voids over the oceans demonstrate the need dramatically. Indeed, it is these large data gaps which provide the essential rationale for all global satellite observations, and in particular, for the major efforts exerted around the world to obtain wind data from cloud tracks (i.e., cloud track winds or CTW) using the global constellation of GEOS. During the recent Global Weather Experiment (GWE), a concerted effort was also made to supplement the CTW's by constant level balloons, regular commercial aircraft reports, and a limited number of wide body aircraft equipped with inertial navigators and ASDAR (Aircraft to Satellite Data Relay) systems, among others. Although the analysis of the GWE data has only recently begun, the available evidence is already quite impressive that the winds provide significant improvements in both objective wind analyses and the forecasts. This is particularly noteworthy because satellite temperature soundings have been available for about a decade and only recently has it been generally accepted that they provide increased forecast skill, although not nearly as great as had been expected. In fact, it was the generally modest improvements which were at the source of the controversy as to the utility of the temperature soundings until it was shown that they provided critical data in particular

regions and weather situations (Atlas, 1979). Space does not allow the review of the nature of the controversy surrounding the utility of satellite temperature soundings.

The basis for placing so much reliance on the satellite temperature soundings was due, in large part, to the assumption that they would define the mass field and this in turn would define the wind field with sufficient accuracy. It was recognized, however, that this would not be the case in the tropics where the coriolis force is small, the pressure gradients are weak, and the geostrophic wind relations break down. The tropical constant level balloon observations were aimed at overcoming this limitation. But the tight relationship between the wind and mass fields also breaks down in some of the most critical situations; that is, when either the curvature of the isobars is so great or the pressure tendencies are so large that the wind does not have time to adjust to balance with the mass field. Then strong ageostrophic wind components occur which can have dramatic effects upon the evolution of the weather system.

This is illustrated in Figure 1a and b for the 850 mb level on Jan. 13, 1979. This shows such an ageostrophic current, marked by the large arrow. In this case, the current is advecting cold dense air directly into the northern portion of an intense cyclone. This contributes to large height rises at this level and below, and large height falls in the upper levels. As a result, the original cyclone (Fig. 1a) fills, and a new cyclone (Fig. 1b) forms downstream within 12 hours where upper level divergence becomes maximized. Cold air injections such as these occur frequently during the winter months and contribute to major modifications of synoptic scale systems. Accurate specification of both the wind and temperature fields is required to account for their dynamical effect within a numerical model.

Even if it is assumed that the winds were everywhere in balance with the mass field, the errors in temperature measurements imply errors in the derived winds and conversely. In Figure 2 we show the layer mean temperature errors resulting from an assumed but reasonable error profile for winds, using the thermal wind equation and horizontal resolutions of 200 and 400 km. The wind

error profile shows the RMS deviations of the rawinsonde winds from the best fit objective analysis done with all available data for the GWE period Jan. 9–14, 1979. Since the objective analysis does not necessarily represent the "truth," the actual errors are probably somewhat smaller; rawinsonde wind errors are actually reported to average about 1.5 m sec^{-1} in the troposphere. Note that since the thermal wind equation relates the winds to the horizontal temperature gradient, the equivalent temperature errors on the right of Figure 2 represent the relative errors corresponding to the indicated resolutions and not the absolute errors. For 200 km horizontal resolution, Figure 2 indicates equivalent RMS relative temperature errors between 1 and 1.5°K; on average, the wind error in m sec^{-1} is 2 to 2.5 times the temperature error. The errors double for 400 km resolution. Of course, these results only provide an estimate of the accuracy required in measuring temperature gradients and thus reflect the necessary precision of temperature measurement from one point to another. Except in cases of sharp gradients of cloud coverage, which contaminate the temperature retrievals, it is believed that present passive sounders do in fact measure temperature gradients better than indicated by the errors shown in Figure 2. This highlights the importance of using the temperature gradients rather than the absolute values under some circumstances, especially on the regional scales.

In order to provide an indication of the required absolute accuracy in temperature measurement to that for wind measurement, we can only refer to GCM simulation experiments such as those reported by Jastrow and Halem (1970). The former introduced random wind errors of various magnitudes and found that an RMS wind error of 2 m sec^{-1} is equivalent to an RMS temperature error of 1°C. Kasahara and Williamson (1972) generally concur with this finding in temperate latitudes but note that larger wind errors ($\sim$3 m sec^{-1}) occur in the tropics, thus supporting the need for direct wind measurements in the tropics. They conclude that:

"The observing system of wind at least at two levels in the tropical belt (25°N–25°S) and at all levels in the equatorial belt (10°N–10°S), together with infrared temperature observations over the globe, is almost the minimum requirement."

10

The Joint Organizing Committee's (JOC) Tropical Wind Experiments were also formulated to determine the minimum observing system necessary to satisfy the GARP requirements for a wind error of 2m sec^{-1} in the tropics. The findings with the GFDL model by Gordon et al., (1972) are illustrated in Figure 3. In Experiment I simulated temperature profiles were inserted into the model with errors within the GARP data requirements. Experiment II consisted of data from Experiment I plus two levels of wind data in the tropical zone simulating wind vectors derived from geostationary cloud images. In Experiment III detailed vertical wind profiles for the equatorial zone were inserted in addition to the data in Experiment II, simulating dropsonde data from a carrier balloon system.

The findings of Gordon et al., were that:

(a) Wind errors obtained from temperature insertion alone exceed the GARP error limits.

(b) The addition of two-level wind data (850 and 200mb) in the tropics significantly improved the wind determination at all latitudes (i.e., the wind information propagates from the tropics to extratropical latitudes).

(c) With two-level tropical wind data added, the wind errors in the tropics still exceeded the GARP error limits.

(d) With dropsonde wind data added in the equatorial zone, the wind errors in the tropics were reduced below the GARP limit of 2m sec^{-1} for tropical winds.

These results illustrate the potential importance of tropical wind data for mid-latitude numerical weather prediction.

It is now possible to make some reliable statements about the various wind measuring techniques used during the GWE. Figure 4, corresponding to wind measurements taken during Jan. 9-14, 1979 shows the RMS fit of each of the wind systems to all the objectively analyzed wind data. The most accurate wind systems are the NAVAIDS, the shipborne rawinsondes in the tropics. The conventional land based radiosondes show somewhat larger errors, due in part to the stronger

11

winds at higher latitudes. Next to the rawinsonde winds in accuracy are the NOAA/NESS cloud track winds, and in the upper troposphere, the ASDAR winds. Both the Japanese and European CTW's show significantly larger errors than the NESS CTW's above the 700mb level. This is due in large part to the better height assignments of the CTW's by NESS and shows the importance of measuring cloud heights either by lidar or stereo techniques as noted earlier.

At this time, there have been very few studies of the impact of actual wind observations on forecast skill. Tracton et al., (1979) performed one such study using NESS CTW's and reported a definite improvement in the 84 hour predicted wind fields. Moreover, they found that the initial objectively analyzed wind fields with CTW's showed the following: (1) large differences (up to 30 to 40m/sec) between SAT and NOSAT winds in the upper troposphere and lower stratosphere in tropical regions and the southern hemisphere; (2) smaller but significant differences in temperate latitudes over the oceans; and (3) generally more intense weather systems with SAT winds. We anticipate many more such impact results emanating from the GWE analyses now underway.

Finally, the value of measuring surface winds over the ocean as has been done with the SEASAT radar scatterometer should be noted. Figure 5 illustrates a segment of the oceanic surface wind field derived from the SEASAT scatterometer superimposed upon the satellite cloud patterns. The inset table shows the results of a 72 hour forecast using the GLAS GCM in which simulated SEASAT winds, with realistic error statistics, were included as initial conditions (Cane, et al., 1980). The results show reductions in the RMS errors of the surface pressure in all regions except the tropics, by 10 to 20%.

We may summarize the above as follows:

(1) Wind measurements are more important than temperature soundings wherever the winds are not in balance with the mass field. This means that they are required to faithfully predict the smaller scale systems at all latitudes, and all scales in the tropics. For the larger scales in mid-latitudes, temperature data are probably more important provided they are accurate to about $\pm 1°C$ RMS.

(2) Even relatively crude satellite wind data (e.g., CTW's) show major real differences at the higher levels in the tropics and southern hemisphere, and smaller but significant differences (i.e., generally more intense weather systems) at higher latitudes.

(3) Forecast simulations using wind data in the tropics and surface wind data over the oceans, show significant increases in predictive skill; one forecast study utilizing actual satellite CTW's confirms such expected improvements.

(4) GCM simulation studies show that an RMS wind error of $2\,\mathrm{m\,sec^{-1}}$ is equivalent to an RMS temperature error of about 1°C outside of the tropics. Thus, a wind system which could achieve such accuracy would be equivalent to the best that is possible by any passive temperature measurement system now available or under consideration. Nevertheless, the prevailing view is that both temperature and wind data are required outside the tropics. It is possible that a DIAL lidar temperature profiler may achieve temperature accuracies of about 1°K (see Section 6).

5. AIR-SEA INTERACTION AND THE PLANETARY BOUNDARY LAYER

The subject of air-sea interactions is of paramount importance in relation to weather and climate on all space and time scales. Some examples of these are: (1) land-sea breezes and their effects on local cloudiness and convective precipitation; (2) the formation of fog and cloud streets over the cold sea and coastal regions and their effects on the radiation budget; (3) cold season cyclogenesis off the eastern continental coasts due to the sensible and latent heating and moisture supply from the oceans, and (4) the evident influence of anomalous sea surface temperatures on regional and global climate on time scales of weeks to months and possibly longer. And of course, in order to achieve a climate predictive capability, the interactions between the atmosphere and oceans will have to be properly parameterized in GCM's. These are but a few of a much longer list of scientific problems which must be addressed.

The intense interest in this subject is typified by a wide range of activities and documents, for example, the report of the JPL-Scripps Workshop on Air-Sea Interactions (NASA, 1980b). Perhaps

one of the most noteworthy conclusions of that report is that the prospects for the direct measurement of the fluxes of heat, moisture and momentum from space are not promising. We suggest that this conclusion is attributable to the fact that the general approach to satellite measurements has been to try to replicate by remote sensors the measurement capabilities of in-situ sensors. Such an approach is undoubtedly doomed to failure since, from space, there is no conceivable way to measure all the required parameters in the few tens of meters above the sea. However, there are large regions of the world and major fractions of the year during which the net fluxes can be inferred from the behavior of the clouds produced as a result of the heat and moisture fluxes. In what follows, the basic approach will be outlined. Details will appear in a forthcoming paper (Atlas et al., 1980).

The point of departure for this concept is the TIROS-N IR (11μm) picture in Figure 6. This shows cloud streets oriented NNE-SSW along the wind direction during a very cold outbreak on Feb. 17, 1979. The color-coded photo shows land and surface air over Long Island, N.Y. of 260°K (-13°C). This cold air streams south over the warmer oceans and is warmed and moistened until clouds form about 100km south of Long Island. From there southward, the increased heating from the sea continues to warm the boundary layer and the clouds grow higher and colder reaching their coldest temperatures of -22°C at about 38°N latitude. Southward of this latitude, the temperatures start to increase again; although this would appear to signify decreasing cloud top heights, it will be seen that this in fact is not the case. IR temperature cross sections corresponding to the N-S (No. 1) and E-W lines (2 and 3) on Figure 6 are shown in Figure 7. These show detailed temperature features of the land, sea, and clouds. In particular, the N-S section No. 1 shows that temperatures of the clouds at the northern edge of the streets are only slightly colder than the SST indicating that they are at very low altitude. Also, where the temperature fluctuates sharply, their amplitude is slightly less than the spread between the SST and the cloud top temperature, due to the partial cloud filling of the holes.

14

The physical situation is shown schematically in Figure 8 where the temperature profiles are shown on the left and a cross-section of the cloud profile along the cloud street is shown on the right. The thick solid curve on the left marked 0 resembles the sounding just as it leaves the coast and is marked by a slightly stable lapse rate from the surface upward to a sharp inversion. In traveling over the slightly warmer coastal waters, the lower level air is heated and moistened from below until clouds form at point A. In such cold air, the saturation vapor density will be very small so that only a slight moistening is required to produce condensation, and the cloud bases may be extremely low. The temperature sounding at point A is shown by the thin solid curve A on the left. Above its intersection with the initial sounding, the air is essentially unmodified and so it follows the initial temperature profile. We may estimate the sounding at A (i.e., first cloud formation) very closely by assuming a dry adiabat from the cloud top temperature down to the surface. Except for a small superadiabatic layer of a few tens of meters or less, the net heat given up by the ocean to the air is given simply by the area between soundings 0 and A.

Analogously, the moisture density at A can be estimated closely by finding the saturation vapor density at the temperature corresponding to the level of first cloud formation, and assuming that the air is well mixed from there down to the surface. The moisture given up to the air from the sea is then the difference between this measure and the mean vapor density in the column below cloud base in the land air.

Estimates of the sensible (S) and latent (M) heating between the coast and point A can then be made from the relations

$$S = (\Delta \overline{T}) \rho c_p \qquad (1)$$

and

$$M = (\Delta \overline{q}) \rho L \qquad (2)$$

where $(\Delta \overline{T})$ is the change in average temperature and $(\Delta \overline{q})$ is the change in average vapor mixing ratio in the layer in question, ρ is air density, c_p is the heat capacity of air at constant pressure,

and L is heat of condensation. In the case of Figure 6, we find an average heating rate of 340 watts m^{-2} over the coastal waters between Long Island and the cloud edge, using a wind speed of 10 m sec^{-1} measured by an ocean buoy located close to the cloud edge. It should be noted that the heating rates are often much larger in the fall and winter over the coastal waters of the southeast U.S. Indeed, Henry and Thompson (1976) compute a heating rate of 1.6 Kw m^{-2} in the 3 hours of transport between Bay St. Louis, Mississippi and the edge of the cloud streets during a cold outbreak over the Gulf of Mexico on November 24, 1970.

Returning to the schematic diagram in Figure 8, we see that as the air is heated further between points A and B, the cloud tops extend to the base of the inversion. This is the coldest point in the lower level sounding; assuming the cloud top temperature to be equal to the environmental temperature, point B on the clouds also represents the coldest cloud temperature. Proceeding from B to C to D, warming continues and the cloud tops continue to rise to equilibrium with the initial sounding, neglecting minor overshooting and mixing downwards. Thus, the cloud top temperatures begin to increase south of Point B while the tops continue to grow. This is evidently the reason for the coldest temperatures in Figure 6 to occur along about the 38°N latitude line. Finally, at point D, presuming that the air has been heated sufficiently to penetrate the inversion, there is enough buoyancy for clouds to develop suddenly to sharply higher levels. This did not occur in the case of Feb. 17, 1979, but is evident on many other occasions. In short, the points of initial cloud formation (A), coldest cloud top temperature (B), and the initiation of sharply higher clouds (D) are distinct fiducial markers which closely indicate the nature of the low-level soundings below the inversion and the transformations which must have taken place. These provide the essential information needed to compute the heating rates.

It is clear from the prior discussions how the observations can be used to compute both the sensible and latent heating along the cloud streets. Of course, once the clouds attain significant depth, the heating equations (1 and 2) have to be altered to account for the moist adiabatic lapse rate through the clouds. This is readily done; the mathematics is described in Atlas, et al., (1980).

16

Until now, the assumption has been implicit that the initial temperature sounding 0 as the air leaves the land is known and, except for modifications in the convective boundary layer, that the temperature profile remains constant above as the air advects over the sea. Unfortunately, these assumptions may not be valid, not only due to the inadequate time and space coverage of the coastal radiosondes, but because of probable changes in the sounding. This is where the lidar comes into play. The lidar, mounted on an aircraft in the near term and ultimately on a spacecraft, will provide excellent measures of the cloud tops while the passive IR radiometer (Advanced Very High Resolution Radiometer-AVHRR) on TIROS-N measures cloud top temperatures. Of course, the latter also provides a good measure of sea surface temperatures (SST) in cloud free regions and in the holes between cloud streets. This is especially true over the coastal waters in the case of the very cold and dry outbreaks where corrections for water vapor absorption are small or negligible. Even without SST, however, the lidar and AVHRR provide all the information required to compute the heat and moisture fluxes.

In order to confirm the estimates of moisture flux deduced as described above, passive microwave sensors in the 18, 21, and 37 GHz bands also may be used. For example, it has been shown (Prabhakara, private communication) that the difference between the 21 and 18 GHz brightness temperatures over the sea are related to the column integrated water vapor content by

$$(T_{21} - T_{18}) = 5 + 6.5 \int_0^Z q \, dz \qquad (3)$$

where q is the absolute vapor density and the integral represents the total columnar amount in $g \, cm^{-2}$. In cloud free regions over water the effective top of the vapor column may be taken as the top of the convective boundary layer, which should be readily detected as a discontinuity in the aerosol backscatter profile seen by lidar. When clouds form, we can infer the columnar cloud liquid water content from the difference in brightness temperatures between either the 18 or 21 GHz and the 37 GHz channel, and use the lidar cloud top measurement to determine the average water content within the cloud layer. In any case, the basic principle involved is to measure differences

in both vapor and cloud water along a trajectory following the low level winds and to use the lidar to determine the heights over which these differences occur on the assumption that all the significant changes in moisture occur within the PBL in the case of cold air outbreaks.

Finally, we note that the combined lidar–IR radiometer temperature–height profile along the cloud streets, as noted above, would provide an excellent high resolution temperature profile corresponding to that in the unmodified air before it leaves the land. This assumes, of course, that there is no appreciable modification of the sounding above the convectively active layer. Even though some modification may occur as a result of mixing across the inversion, our inability to obtain high resolution soundings with any passive methods recommends the approach as a substitute. This approach may also be used in any situation in which the cloud height is in thermal equilibrium with the environmental temperature. An analogous method has been proposed by Hasler and Adler (1980) using stereo height and IR temperature measurements from geosynchronous satellites. This is just one more example of the way in which we must aim to exploit the combination of the unique capabilities of remote sensors and physical insight to retrieve significant meteorological information, and to overcome our disposition to duplicate the in-situ capabilities of such measurements systems as the radiosonde.

6. TEMPERATURE, PRESSURE, AND MOISTURE PROFILING

It has already been noted that winds and the atmospheric state variables, temperature, pressure, and humidity, are the basic parameters required in all prediction methods. Indeed, they are fundamental to studies of virtually every meteorological phenomenon on every space and time scale. A measure of their importance is the large investment in the global network of radiosonde stations and satellites attempting to measure them from space over the oceans and unpopulated regions of the globe.

The interest in improved space measurements of temperature and humidity derives from two essential factors: (1) the accuracy of present passive remote temperature sensors, e.g., High

Resolution Infrared Spectrometer (HIRS), is now limited by RMS errors of the order of 1.5 to 3°C depending upon height, and vertical resolution no better than 5 km with very little useful information in the surface layer; (2) humidity soundings are extremely crude in both accuracy and resolution and provide very little useful information in the lower layers. The situation would be improved with the proposed new Advanced Meteorological Temperature Sounder (AMTS). A comparison of the simulated temperature accuracy of the AMTS and HIRS is shown in Figure 9. While the AMTS comes close to satisfying the temperature accuracy requirement of ±1°C RMS, its vertical resolution is inherently limited to about 4 km. Also, like all passive temperature sounders, its weighting functions extend over the entire atmosphere and the data must be inverted to retrieve the temperature profile. As a result, the data obtained depend heavily on the shape of the initial guess profile, and the presence of unknown temperature structure (e.g., inversions) can cause large errors. On the other hand, simulations of the accuracy and resolution achievable by a lidar temperature sounder in the troposphere (see below) indicate RMS errors less than 1°C and a vertical resolution of 2 km; the combination of higher accuracy and resolution is expected to be of considerable value. Moreover, a lidar temperature sounder provides relatively direct measurements of temperature at known heights without the need for inversion. Indeed, the accuracy and resolution of a lidar sounder is currently limited only by the energy available for a measurement, and vertical resolution as high as 100 m is planned for aircraft flights in the near future.

The basic lidar concepts for measuring temperature, pressure, and moisture are DIAL or modified DIAL techniques. While the basic methods are well known to the specialists in the field, we review them briefly below.

6.1   Differential Absorption Lidar for Integrated Path and Differential Ranging (DIAL) Measurements

A dual frequency lidar is used for an integrated path differential absorption measurement. One frequency is chosen on a portion of the resonant absorption feature which is to be measured (i.e., on-line). A second nearby frequency, which suffers minimal resonant absorption, but which has

nearly identical attenuation due to various scattering and continuum absorption processes is used as the reference. The ratio of the signal returns from range R at the on-line and off-line frequencies, $E_L(R)$ and $E_r(R)$ respectively, may be formulated to yield the integrated optical depth

$$-(1/2) \ln \left\{ \frac{E_L(R)/E_r(R)}{E_L(O)/E_r(O)} \right\} = \int_0^R K \, dr \tag{4}$$

where the return signals are normalized for transmitter output at the two frequencies as given in the denominator by $E_L(O)$ and $E_r(O)$. In order to obtain vertical resolution, the dual frequency measurements are made simultaneously using a combination of aerosol and molecular backscatter from two successive ranges R and $R + \Delta R$. The difference in optical depths for these measurements, ratioed to the range element ΔR, then yields the net absorption coefficient for the volume element between the two ranges. In DIAL methods, the absorption coefficient is normally used to obtain the concentration of the on-line absorbing species. However, we shall show that it may also be used to obtain the temperature profile.

6.2 Lidar Pressure Measurements

The theory of lidar measurements of pressure has been given by Korb, et al., (1977a,b; 1979a). An integrated path differential absorption experiment is conducted as was discussed above. A pressure sensitive measurement is obtained using two frequencies; one located in the trough region between two very strongly absorbing oxygen lines in the "A" band region near 0.760 μm as shown in Figure 10a, and a second in a nearby region just off the oxygen "A" band near 0.7590 μm. The two curves in Figure 10a correspond to the cumulative extinction by oxygen for a two way path from outer space down to the surface and 4 km, respectively. The inset equation shows that this cumulative extinction is proportional to the square of the pressure at the measurement level, either the surface, the cloud tops, or the height of the atmospheric layer which is used to range on.

6.3 Lidar Temperature Measurements

A two-wavelength DIAL lidar technique may also be used to measure the atmospheric temperature profile (Korb et al., 1979b). A highly sensitive temperature measurement is obtained by

20

locating one wavelength at line center in the oxygen A band near $0.768\,\mu m$ as shown in Figure 10b with a second reference wavelength located within $0.1\,nm$ in order to normalize out the effects of atmospheric scattering and continuum absorption common to both wavelengths. At the former wavelength the absorption coefficient is very sensitive to temperature through the Boltzmann distribution so that the measurements using backscatter from the atmosphere at two adjacent heights provide a determination of the mean temperature of the layer. See the inset equation in Figure 10b showing the quantitative relationship.

6.4 Water Vapor Measurements

Water vapor is measurable by a straightforward application of the DIAL technique. In a manner similar to the temperature method shown in Figure 10b, one frequency is selected to correspond to a measurement at the center of a water vapor line in the region near $0.724\,\mu m$ with a second nearby reference wavelength. As shown by the equation in Figure 10b, the measured absorption coefficient, K, is directly proportional to the water vapor mixing ratio averaged over the measurement layer.

6.5 Performance Simulations and Experiments

Simulations of the performance of the lidar temperature, pressure (Korb et al., 1979a, b) and water vapor (Wilkerson and Schwemmer, 1979) techniques have been conducted both for the Shuttle and ground based systems. The assumed measurement conditions are summarized in Table 3. The computed accuracy for the Shuttle-based temperature profiles is shown in Figure 11. We see that the expected error is slightly greater than $0.5°C$ near ground level and increases gradually to about $1°C$ near $10\,km$ altitude. For measurements above $10\,km$, the stronger absorption associated with other lines would produce similar results.

The simulated results for the accuracy of the surface pressure measurement, shown in Figure 12, assume a 150 shot average which corresponds to a horizontal resolution of $100\,km$. With such a system, surface pressure would be measurable to an accuracy of 0.2%. Also, cloud top pressures

Table 3

Assumed Lidar Characteristics for the Various Techniques to Measure Temperature,
Pressure, and Humidity from a Spacecraft at 200 km Altitude

Lidar Parameter	Measurement				
	Temperature Profile	Pressure Profile	Surface Pressure	Cloud Top Pressure	Moisture Profile
On Line (μm)	0.7690	0.7600	0.7600	0.7600	0.7243
Reference (μm)	±0.0001	0.7592	0.7592	0.7592	±0.0001
Pulse Energy (J)	0.1	0.05	0.05	0.05	0.05
Pulse Width (nsec)	<20	<20	<20	<20	<20
Pulse Rate (Hz)	10	10	10	10	10
Pulses Averaged	700	700	150	25	60
Horizontal Resolution (km)	500	500	100	16	40
Collector Size (m^2)	1	1	1	1	1

could be measured to better than 0.2% over a broad range of altitudes with a 25 shot average and horizontal resolution of 16 km.

The results of pressure profiling simulations are shown by the solid curve in Figure 12. For a horizontal resolution of 500 km, the accuracy is close to 0.3% (i.e., 3 mb) near the surface and rises slowly to about 0.4% (i.e., 2 mb) at 5 km. Water vapor lidar simulations for the Shuttle (Fig. 13) show that tropospheric water vapor profiles can be measured to accuracies of better than 10% with 1-2 km vertical resolution up to 10 km. The solid and dashed curves correspond to wavelengths of $0.7243 \mu m$ and $0.7187 \mu m$, respectively, while the three different curves correspond to the vertical resolutions. Weak absorption lines are used when probing regions of high humidity, as in the lower troposphere, and stronger lines are used to probe regions of weak humidity as in the upper troposphere. Even stronger line strengths, such as are found in the $0.94 \mu m$ H_2O band, can be used to measure stratospheric water vapor to accuracies of 20-30%.

The simulations were conducted with laser systems within the current state of the art. It should be noted that recent advances in detectors for the $0.76 \mu m$ region currently provide nearly an additional factor of two improvement in quantum efficiency. It is also expected that advances in the technology in the next few years will provide increased transmitter power, efficiency, and longer life. When these are realized, we expect that results such as those shown in the simulations will be achievable from higher orbits and with less averaging, thus permitting measurements at higher horizontal resolution, and longer duration space missions.

Laser measurements of both temperature and pressure have recently been demonstrated (Kalshoven et al., 1980; Korb, 1980). These experiments have been conducted in a continuous wave (CW) mode using one ultra-high resolution laser for the on-line measurements and a somewhat lower resolution laser for the off-line measurements. The experiment was used to make measurements over a 2 km round trip atmospheric path between the laser and a fixed target. Initial temperature measurements, as given in Figure 14a, show a noise level of typically 0.5°C and a temperature accuracy of 1°C over a 20°C temperature range. It is believed that the 1°C agreement

between the temperature measured with the laser and those obtained with a thermometer is limited by the use of only a single point measurement for ground truth along the path. In addition, initial pressure measurements have been conducted. The results are given in Figure 14b and show that accuracies of better than 3 mb have been obtained with noise levels as low as 1 mb.

While these ground-based atmospheric measurements were performed using a CW laser system, they nevertheless demonstrate the feasibility of the basic method. Indeed, the path-averaged temperature measurement appears ready for use in a number of important ground-based research and operational applications.

7. AN ALTERNATIVE APPROACH TO LIDAR WIND SENSING FROM SPACE AND A TOTAL SYSTEM CONCEPT

At the present time the primary candidate system for wind sensing from space is CO_2 Doppler lidar (Huffaker, 1978). The latter approach is conceptually sound; however, there are many serious questions concerning its feasibility. These will not be enumerated here for they have been treated by Huffaker and his colleagues. In brief, there are doubts about the required technology in the CO_2 band related to signal to noise ratio and Doppler processing, and the size and pointing accuracy of the telescope. Meteorologically, prime concerns relate to the presence of aerosols in sufficient quantities over the globe to be detectable at 10μm wavelength, to the measurement errors resulting from sharp wind gradients, and to the adequacy of data at 500 km spacing in the presence of small scale systems.

There is far less doubt about our ability to detect aerosols by elastic scatter at wavelengths shorter than 10.6μm, that chosen for the Doppler wind system. For example, the backscatter reflectivity of a typical aerosol size spectrum is about 15 times greater at 0.7μm than it is at 10.6μm (Huffaker, 1978). Thus it seems natural to consider the possibility of estimating winds from the displacements of the aerosol patterns between two consecutive observations rather than from the Doppler shifts.

24

A possible conceptual approach is illustrated in Figure 15. The system is comprised of two beams; one canted forward, and the other toward the rear at nominal angles of 45 degrees. For an orbit of 700 km altitude, the rearward beam would view the same area previously seen by the forward beam about 3.3 min earlier. Both beams are scanned perpendicular to the orbital path covering a nominal swath width of say 10 km, thus covering a square of 10 km on a side in about 1.4 sec. With range gating, one then generates two maps of the aerosol back-scatter signal at each of a multiplicity of heights in the atmosphere separated 3.3 min in time. To determine the winds, the pattern displacement is simply measured by means of any one of a variety of existing techniques. Space-time autocorrelation is probably the preferred scheme. This has been done very effectively in a variety of satellite cloud tracking routines and has also been applied to wind measurements using ground based radar (Rinehart, 1979a,b).

It should be noted that this approach places no great demands on the absolute pointing accuracy of the lidar since the winds are determined from the relative displacement of the echo pattern and not from any absolute reference.

For winds up to $100 \, m \, sec^{-1}$, the displacement in 200 sec would be as large as 20 km, suggesting that the scan area should be increased or the intervals between successive patterns be decreased, especially at the higher levels. The latter can easily be done with the proposed configuration which obtains data either continuously or intermitantly, both ahead of and behind the spacecraft.

The measurement accuracy depends upon the resolution within the scan area. Generally, the more data points within the scan area, the more accurate will be the lag autocorrelation measurement of the displacement vector. Also, assuming a resolution and sample spacing of 100 m, the minimum measurable displacement and the position error will be approximately the same; thus a first guess at the wind error is approximately 100 m/200 sec or $0.5 \, m \, sec^{-1}$. Pattern autocorrelation techniques actually can perform somewhat better than implied by the minimum resolution. In any case, if errors of about $\pm 2 \, m \, sec^{-1}$ are acceptable, a minimum sample spacing of about 400 m is required for 200 sec intervals. This corresponds to an array of 25 x 25 samples per 10 km square

25

which gives a pulse repetition rate of about 450 sec⁻¹. This would not be a terribly demanding requirement on existing laser technology, but the power requirements to obtain adequate measurement accuracy might be. The lidar system would not, however, have to operate continuously at the above repetition rate. For example, if wind measurements are desired at intervals of 200 km, the average rate would be reduced by a factor of 20 to about 22 sec⁻¹. We visualize the use of an on-board processor for the wind computations. Of course, the methodology and accuracy assessments need to be refined in a thorough feasibility study.

Needless to say, a system which maps aerosol patterns could readily map the cloud top topography and reflectivity, and with polarization detection, could also discriminate between ice and water near cloud top.

With a wind measurement system such as that described above, it is now possible to conceive of a total system which measures aerosol profiles, wind, temperature, humidity, and pressure, cloud heights, and cloud top water phase. Indeed, it appears possible to utilize a single basic lidar operating in and near the 0.76μm band with sequential selective tuning to perform the DIAL measurements of temperature, moisture, and pressure as previously described. If 10 sec out of the 200 sec over the 1400 km orbital path are used to make wind measurements at 200 km intervals, 190 sec would be available to make all the other measurements.

Obviously, the total concept may be readily extended to off nadir measurements to fill in the gaps between adjacent orbits. Assuming a 1200 km spacing between polar or sun-synchronous orbits at the equator, and a required longitudinal resolution of 200 km, the measurements would have to be repeated at six cross orbital positions. This would, of course, place increasingly demanding requirements on the lidar power, efficiency, and repetition rate as well as on the data rate of the communications system and the load on the on-board processor.

It should be obvious that the system proposed here for use on a spacecraft may be extended directly to either ground based or aircraft borne applications. Indeed, it is in such modes that they

can be implemented in the near term without major technological developments. Moreover, experience with either a ground or aircraft system will better assure the ultimate success of the spaceborne system. In any case, a ground-based system capable of sounding temperature, pressure, humidity, and winds, even if limited to clear or partly cloudy conditions, would be a major step in supplementing the radiosonde systems by providing virtually continuous sounding data between radiosonde launches. Ultimately, we believe it will be possible to replace the radiosonde completely by a remote sensing system comprised of a composite of passive and active sensors in the optical, infrared, and microwave bands.

While the concepts outlined here in broad strokes require a great deal more study, and some may demand significant technological advances, the prospects of making so many of the fundamental measurements of interest to weather and climate are so exciting that one can only urge that we exert our utmost efforts to bring them to fruition.

8. SUMMARY

This paper reviews the weather and climate requirements for remote measurements of the atmosphere from space, and the potential of meeting these needs by lidar. Several new lidar measurement concepts are also discussed.

The most basic requirements relate to extended range global weather prediction out to a week and climate prediction on time scales of a month to a year. They include all the atmospheric state variables: temperature, pressure, humidity, and winds. These need to be specified accurately at some initial time in order to make predictions of the future state of the atmosphere through the use of numerical regional and global circulation models (GCM's).

Cloud cover and top heights, precipitation, and sea surface temperature are also required for both global weather and climate, while a number of other surface boundary conditions such as albedo, snow and sea ice cover, soil moisture, and aerosols are needed for climate. Many of these surface properties and others, which are sensed passively from space, require lidar measurements

27

of absorbing gases and aerosols in order to make the corrections necessary to produce sufficiently accurate surface measurements. For example, IR measurements of sea surface temperature must be corrected for water vapor absorption, which should be measurable by DIAL lidar.

Aside from the intrinsic importance of tropospheric and stratospheric aerosols in connection with the earth radiation budget, the heights of the aerosol discontinuities which commonly mark the tropopause and boundary layer may be used to improve the accuracy of retrievals of passive temperature and humidity soundings. Also, lidar cloud measurements would greatly aid the height assignment of satellite cloud tracked winds.

Perhaps the greatest weakness in the present global observing system is in wind measurements. The paper reviews the arguments for and accuracies required of such measurements. Wind data are needed wherever the winds are not in balance with the mass field; i.e., for the smaller scale weather systems at all latitudes, and for all scales in the tropics. Even crude wind observations, such as the satellite cloud track winds, show major real differences in objective analyses at the higher levels in the tropics and southern hemisphere, and smaller but significant differences at all latitudes; the addition of wind data generally shows the weather systems to be more energetic. Forecast simulations using wind data in the tropics and surface wind data over the oceans show significant increases in skill. This has now been confirmed in limited forecast experiments with satellite cloud winds. GCM observing system simulation studies also indicate that wind measurements having an accuracy of $\pm 2\,\mathrm{m\,sec^{-1}}$ would be equivalent in impact to temperature measurements of about $\pm 1°C$ accuracy. The concensus view is that direct wind measurements are required in the tropics, but that both wind and temperature data are required at other latitudes.

Special attention is given to the need for regional and global scale measurements or estimates of the fluxes of sensible and latent heat from the ocean to the atmosphere for a variety of weather and climate applications. The prospects for making such measurements from space have generally been found to be grim. However, we propose a method which is applicable during the fall and

winter months when cold continental air streams out over the warmer ocean waters and gives rise to cloud streets in the boundary layer. The combination of lidar measurements of cloud tops and infrared measurements of their temperatures provide all the information required to make reasonable estimates of the heat and moisture fluxes. The combined measurements also provide a high resolution temperature profile through the boundary layer and the capping inversion.

Recent concepts for the use of lidar in a differential absorption (DIAL) mode to measure profiles of temperature, humidity, and pressure from space down to the surface or to cloud tops are also reviewed. Theoretical feasibility studies have been conducted. Making reasonable assumptions about the capabilities of lidars expected to be available in the not too distant future, such space-based measurements are found to be feasible. Expected accuracies for temperature sensing are approximately $\pm 1°C$ RMS with 2 km vertical resolution through the troposphere. Pressure profiling with 1 km resolution is expected to be accurate to about $\pm 0.3\%$ from the surface to 6 km. Water vapor profiling is expected to provide measurements with better than 10% accuracy through the troposphere. Ground based trials using a CW laser over a 2 km two way path to a fixed reflector have already demonstrated a temperature measurement accuracy of $\pm 1°C$ and a pressure accuracy of ± 3 mb. These ground based results indicate the feasibility of making path average temperature measurements in the lower atmosphere which have a variety of important research and operational applications.

We also discuss an alternative concept to the use of CO_2 Doppler lidar for the measurement of winds. The method involves mapping the horizontal displacement of the pattern of aerosol backscatter signals at each of a multiplicity of heights, first as viewed by a forward looking scanning satellite lidar beam, and then viewed by a rearward looking beam some 200 sec later. The spatial autocorrelation of the two successive patterns provides the wind vector. A preliminary estimate of the accuracy indicates errors less than about ± 2 m sec^{-1} assuming a lidar sampling resolution of 400 m, sufficient signal to noise, and a 200 sec interval between successive views.

29

Finally, we propose that a space-based atmospheric lidar be approached as a total system. A DIAL system operating in and near the 0.76 μm band, with selective sequential tuning to allow for temperature, pressure, and humidity sounding, and for wind measurements through aerosol pattern displacements, appears within reach within this decade. Such a system would also provide aerosol backscatter profiles, measurements of cloud coverage, topography, reflectivity, and cloud water phase, among others. The technological advances necessary to bring such a system to fruition are not trivial, but the needs for these measurements are so great, and the prospects of obtaining them so exciting, that they must be pursued vigorously. A ground or aircraft based version of the composite system should be readily implemented in the near term, and would meet a wide variety of valuable research and operational needs even though it would be limited to clear or partly cloudy conditions.

9. ACKNOWLEDGEMENTS

REFERENCES

Atlas, D., S. Chou, P. Hwang, and L. J. Allison, 1980: Estimating the sensible and latent heating of the lower atmosphere over the ocean by satellite cloud observations. NASA Technical Report, In press. (To be submitted to the J. Atmos. Sci.)

Atlas, R. M., 1979: A comparison of GLAS SAT and NMC high resolution NOSAT forecasts for 19 and 11 Feb. 1976. NASA Technical Memorandum 80591, Goddard Space Flight Center, Greenbelt, MD.

Cane, M. A., V. J. Cardone, M. Halem, and I. Halberstam, 1980: On the sensitivity of numerical weather prediction to remotely sensed marine surface wind and temperature data: a simulation study. Submitted to J. Geophys. Res.

Gordon, C. T., L. Umschield, and K. Miyakoda, 1972: Simulation experiments for determining wind data requirements in the tropics. J. Atmos. Sci., 29, 1064.

Hasler, A. F. and R. F. Adler, 1980: Cloud top structure of a tornadic thunderstorm from 3-minute interval stereo satellite images compared with radar and other observations. Preprints, 19th Conference on Radar Meteorology, Apr. 15-18, 1980, Miami Beach, FL, Amer. Meteor. Soc., Boston, MA, 405-412.

Henry, W. K. and A. H. Thompson, 1976: An example of polar air modification over the Gulf of Mexico. Mon. Wea. Rev., 104, 51-59.

Huffaker, R. M., editor, 1978: Feasibility study of satellite borne lidar global wind monitoring system. NOAA Technical Memorandum ERL WPL-37, Wave Propagation Laboratory, Boulder, CO, 297 pp.

Jastrow, R and M. Halem, 1970: Simulation studies related to GARP. Bull. Amer. Meteor. Soc., 51, 490-513.

Kalshoven, J. E., Jr., C. L. Korb, M. Dombrowski, and G. Schwemmer, 1980: CW laser measurements of atmospheric temperature, 10th International Laser Radar Conference, Conf. Abs., Silver Spring, MD.

Kasahara, A and D. Williamson, 1972: Evaluation of tropical wind and reference pressure measurements: Numerical experiments for observing systems. Tellus, 24, 100-115.

Korb, C. L., 1977a: A laser technique for the remote measurement of pressure in the troposphere, 8th International Laser Radar Conference, Conf. Abs. Drexel University, Philadelphia, PA.

Korb, C. L., 1977b: Laser measurement of atmospheric pressure profiles, Proceedings, 31st Symposium on Molecular Spectroscopy, Ohio State University, Columbua, OH.

Korb, C. L., J. E. Kalshoven, and C. Y. Weng, 1979a: A lidar technique for the measurement of atmospheric pressure profiles, Transactions of the American Geophysical Union, Spring, Washington, DC.

Korb, C. L. and C. Y. Weng, 1979b: A two-wavelength lidar technique for the measurement of atmospheric temperature profiles, 9th International Laser Radar Conference, Conf. Abs., Munich, Federal Republic of Germany.

Korb, C. L., 1980: Private Communication, NASA/Goddard Space Flight Center, Greenbelt, MD.

NASA, 1974: U.S. Plan for Participation in FGGE. NASA, Goddard Space Flight Center, Greenbelt, MD.

NASA, 1977: Proposed NASA Contribution to the Climate Program. NASA, Goddard Space Flight Center, Greenbelt, MD.

NASA, 1979: Shuttle Atmospheric Lidar Research Program. NASA SP-433, Washington, DC, 220 pp.

NASA, 1980a: NASA Tropospheric Program Plan (DRAFT). Working Group on Tropospheric Program Planning, NASA, Washington, DC, 210 pp.

NASA, 1980b: Guidelines for the air-sea interaction special study: An element of the NASA Climate Research Program. Jet Propulsion Laboratory, Publication 80-8, Feb. 15, 1980. JPL, Pasadena, CA.

Rinehart, R. E., 1979a: Internal storm motions from a single non-Doppler weather radar. Doctoral dissertation, Department of Atmospheric Sciences, Colorado State University, Fort Collins, CO, 257 pp.

Rinehart, R. E., 1979b: A comparison of internal storm motions determined from a conventional radar and a triple-Doppler system. Preprints, 11th Conference on Severe Local Storms, Oct. 2-5, 1979, Kansas City, MO. Amer. Meteor. Soc., Boston, MA, 523-529.

Tracton, M. S., R. D. McPherson, J. D. Stackpole, A. Thomasell, and M. T. Young, 1979: The impact of satellite derived winds upon NMC's data assimilation system. Preprints, Fourth Conference on Numerical Weather Prediction, Oct. 29-Nov. 1, 1979, Silver Spring, MD. Amer. Meteor. Soc., Boston, MA, 345-350.

Wilkerson, T. D. and G. K. Schwemmer, 1979: 9th International Laser Radar Conference, Conf. Abs., Munich, Federal Republic of Germany.

WMO-ICSU, 1973: The First GARP Global Experiment—Objectives and Plans. GARP Publications Series No. 11, WMO-ICSU Joint Organizing Committee, 107 pp.
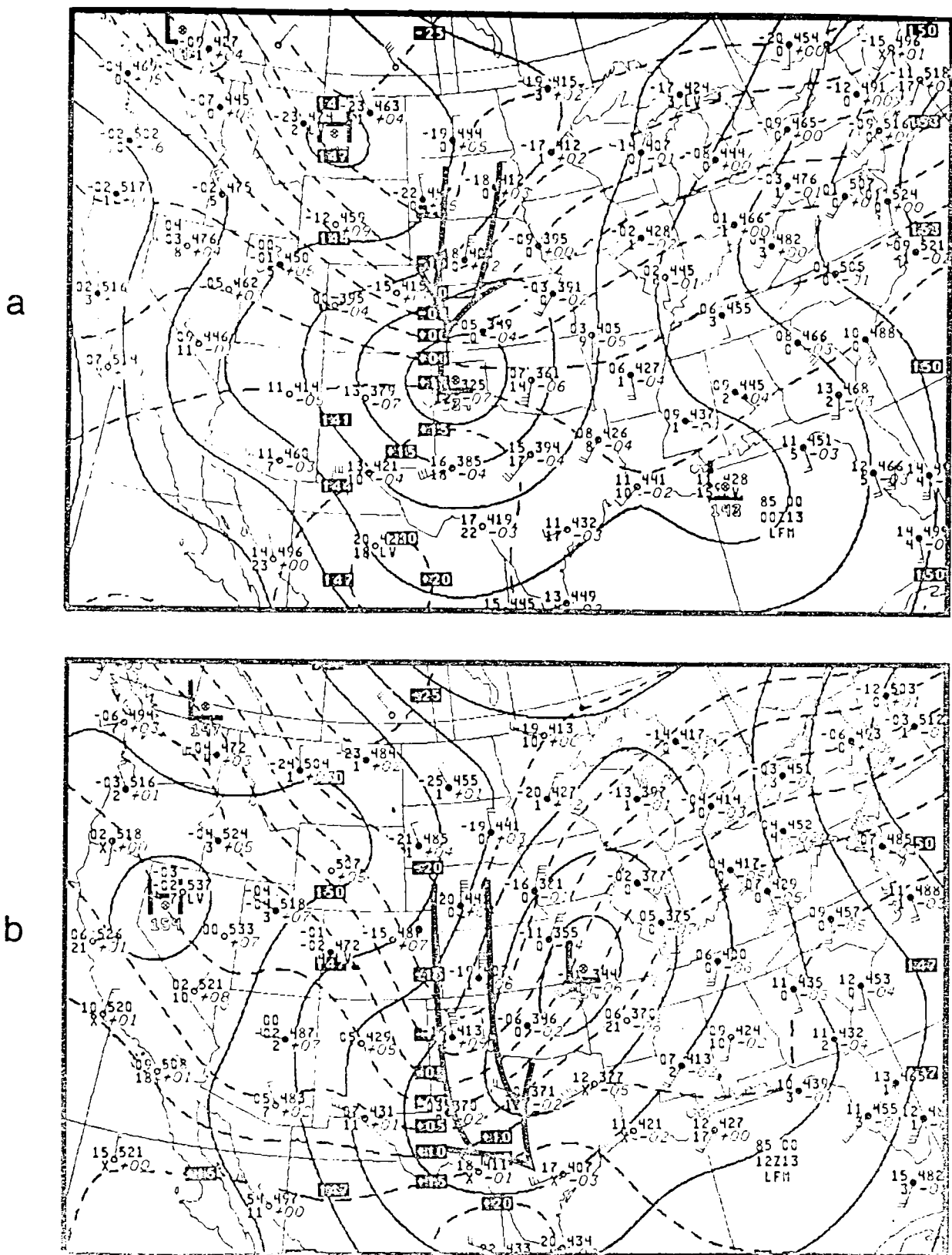
Figure 1. 850 mb analyses for (a) 0000 GMT and (b) 1200 GMT 13 Jan 79. Light, solid lines represent height contours; dashed lines represent isotherms; heavy arrows delineate the cold air injection.

LAYER MEAN TEMPERATURE ERROR RESULTING FROM AN ASSUMED OBSERVATIONAL WIND ERROR USING THE THERMAL WIND RELATIONSHIP

$$\mathbb{W}_{TH} \simeq \frac{R_d}{f}\, \ell_n\!\left(\frac{P_1}{P_2}\right) \nabla_P\, \bar{T}_v$$
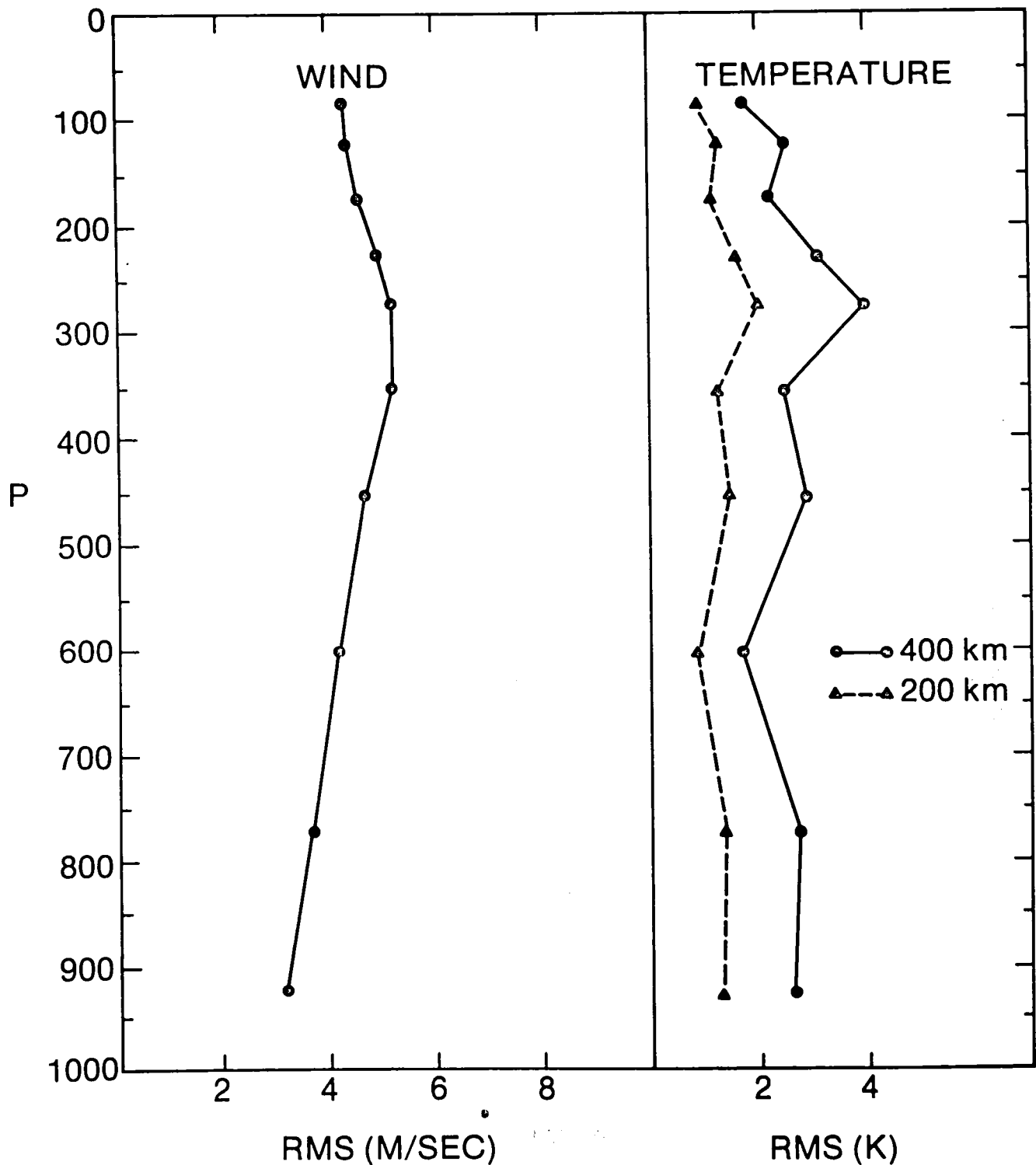
Figure 2. Left—RMS wind deviations of the global network of rawinsonde measurements from the objective wind analyses for the Global Weather Experiment period January 9-14, 1979. Right—Corresponding errors in layer mean temperatures over 200 and 400km horizontal spacing using the thermal wind equation shown at the top. See text.

35

VERTICALLY AVERAGED QUASI-ASYMPTOTIC RMS VECTOR WIND ERROR VERSUS LATITUDE AT DAY 16, HOUR 10, FOR SIMULATION EXPERIMENTS WITH THE GFDL MODEL. ADAPTED FROM GORDON ET AL (1972). I, II, AND III REFER TO "EXPERIMENT" NUMBERS.
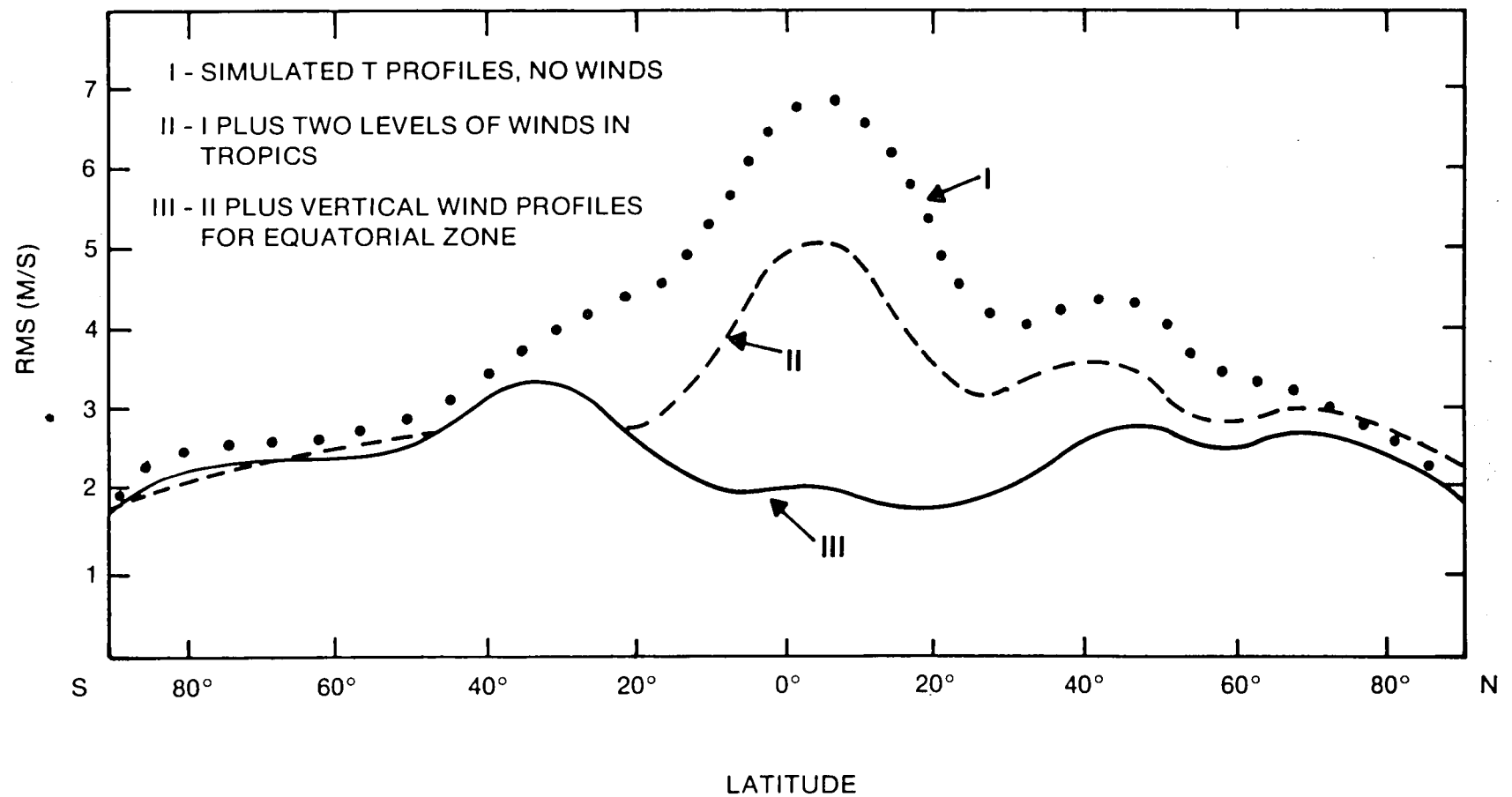
Figure 3. Vertically averaged quasi-asymptotic rms vector wind error versus latitude at day 16, hour 10, for simulation experiments with the GFDL model. Adapted from Gordon et al., (1972).
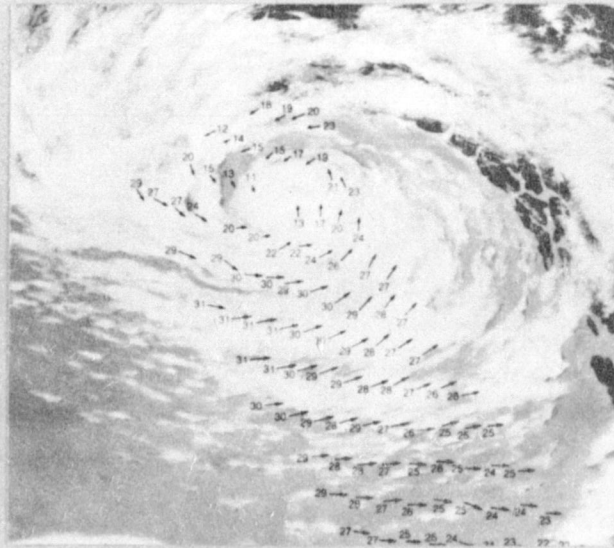
VERTICAL PROFILE OF RMS WIND VECTOR FIT
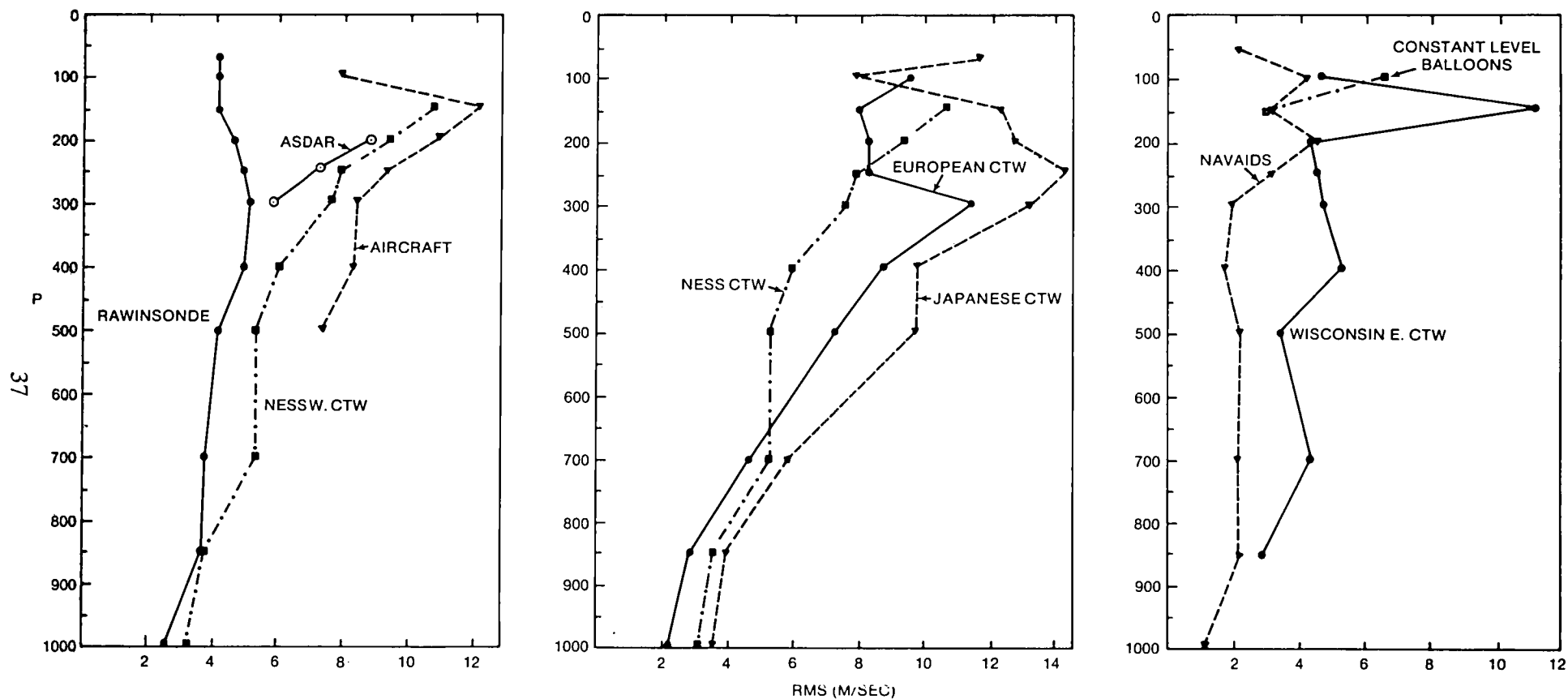
Figure 4. RMS wind deviations from the GWE objective analyses for January 9-14, 1979 corresponding to the various wind measuring systems used during the experiment. CTW corresponds to "cloud track winds." See text for details.

GLOBAL WEATHER SCATTEROMETER WINDS

SEA SURFACE WINDS

SIMULATED IMPROVEMENTS IN FORECASTS

REGION	72 HR SFC PRESSURE FCST % IMPROVEMENT
TROP. OCEAN	4
N. AMERICA	15
N. ATLANTIC	21
N. PACIFIC	20
EURASIA	11

Figure 5. Left—Sea surface winds as measured with SEASAT-A radar scatterometer. Right—Reductions in RMS surface pressure errors resulting from the use of the surface winds in a simulated 72 hour forecast. (Cane et al., 1980.)
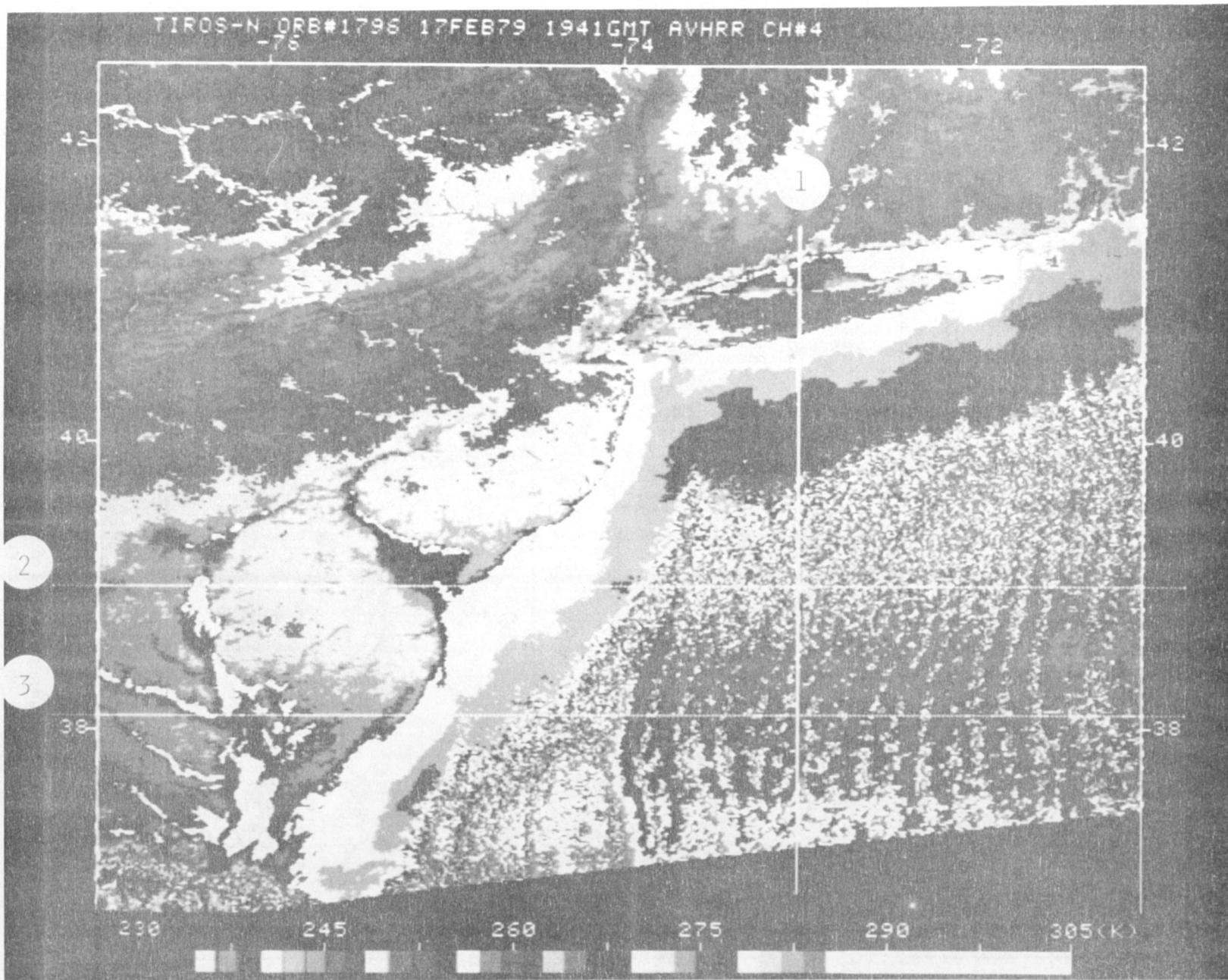
Figure 6. TIROS–N AVHRR IR channel display of coastal ocean temperatures and cloud top temperatures of cloud streets during a cold northerly outbreak on 17 February 1979. Time 1941 GMT. Temperatures are shown by color scale at bottom of figure. Lines marked 1 (N–S), 2 and 3 (E–W) represent the sections corresponding to the temperature profiles in Figure 7.

AIR-SEA INTERACTION
TEMPERATURE CROSS-SECTIONS
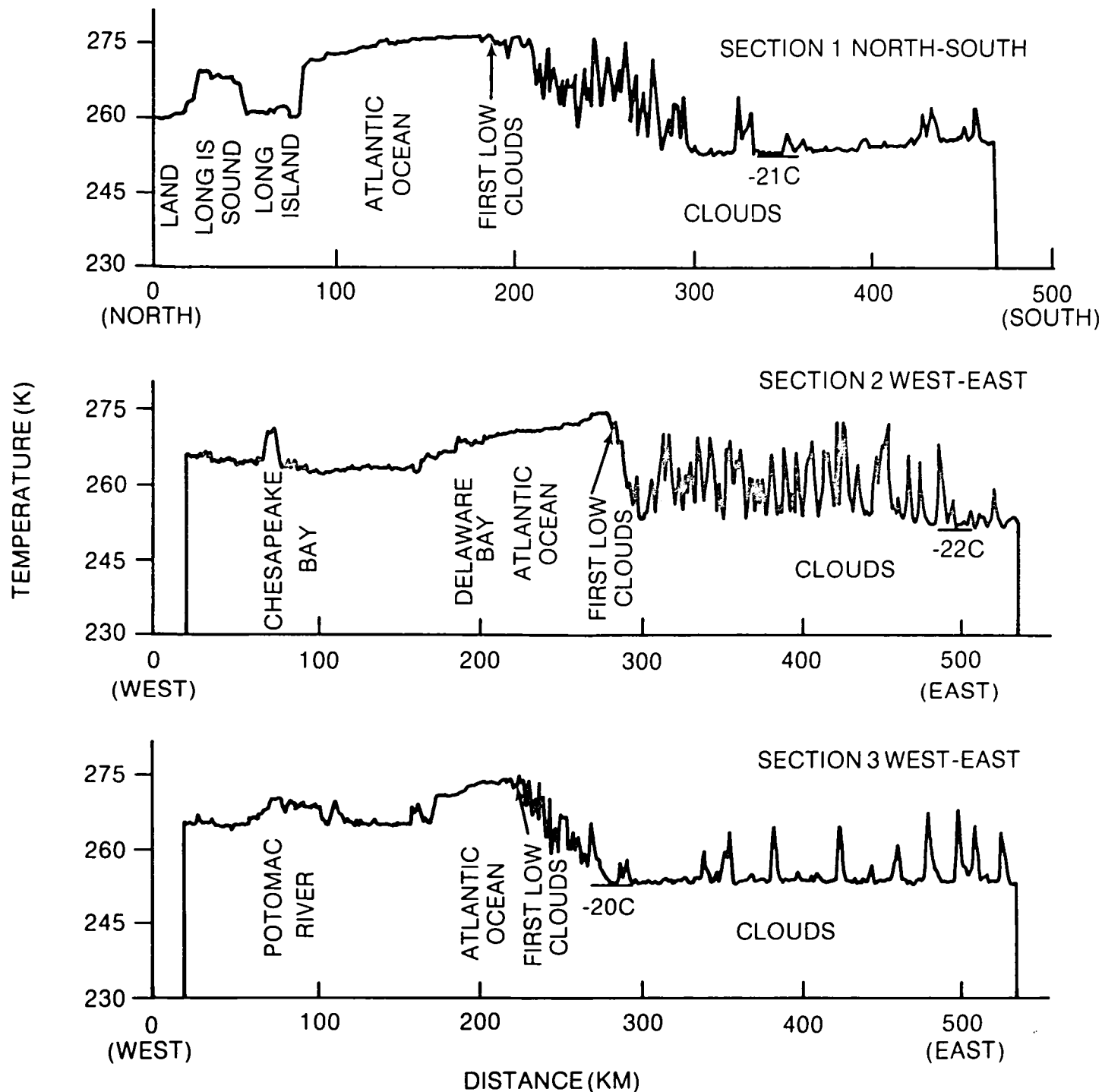### 17 FEB 79   1941 GMT   TIROS-N AVHRR   CH4

Figure 7. IR surface and cloud top temperature profiles corresponding to the sections shown on Figure 6. Top—Section 1, oriented N-S, along the wind and cloud-street direction shows the onset of clouds approximately 100km south of Long Island, NY. Fluctuating temperatures represent openings between clouds through which the sea surface temperature is sensed. Middle—E-W temperature profile corresponding to Section 2 on Figure 6. Various features are indicated. Bottom—E-W temperature profile corresponding to Section 3 on Figure 6. Note that cloud tops are now slightly warmer (-20°C) than the coldest (-22°C) shown in Section 2 and that there are fewer "holes" in-between cloud streets.

40

AIR-SEA INTERACTIONS

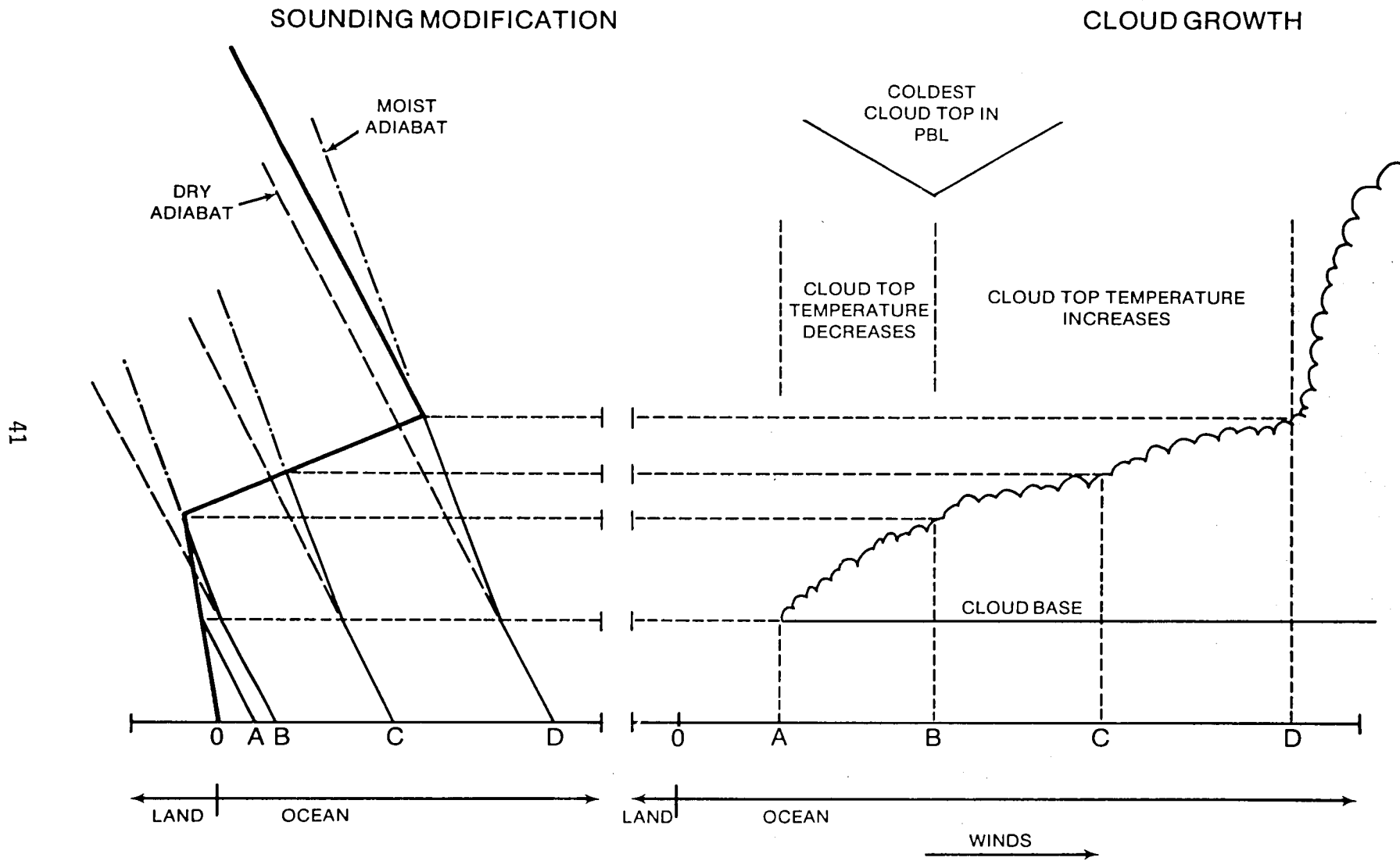SOUNDING MODIFICATION   CLOUD GROWTH

Figure 8. Schematic vertical cross-section of the initiation and growth of a cloud street in cold outbreak over warm ocean along the wind direction, and the manner in which the cloud top temperatures may be interpreted in terms of the original temperature sounding at the coast (0). Temperature soundings A to D correspond to positions marked on cloud section and depict the heating of the boundary layer. See text.

AMTS SIMULATION STUDY
RMS MEAN LAYER TEMPERATURE ERRORS
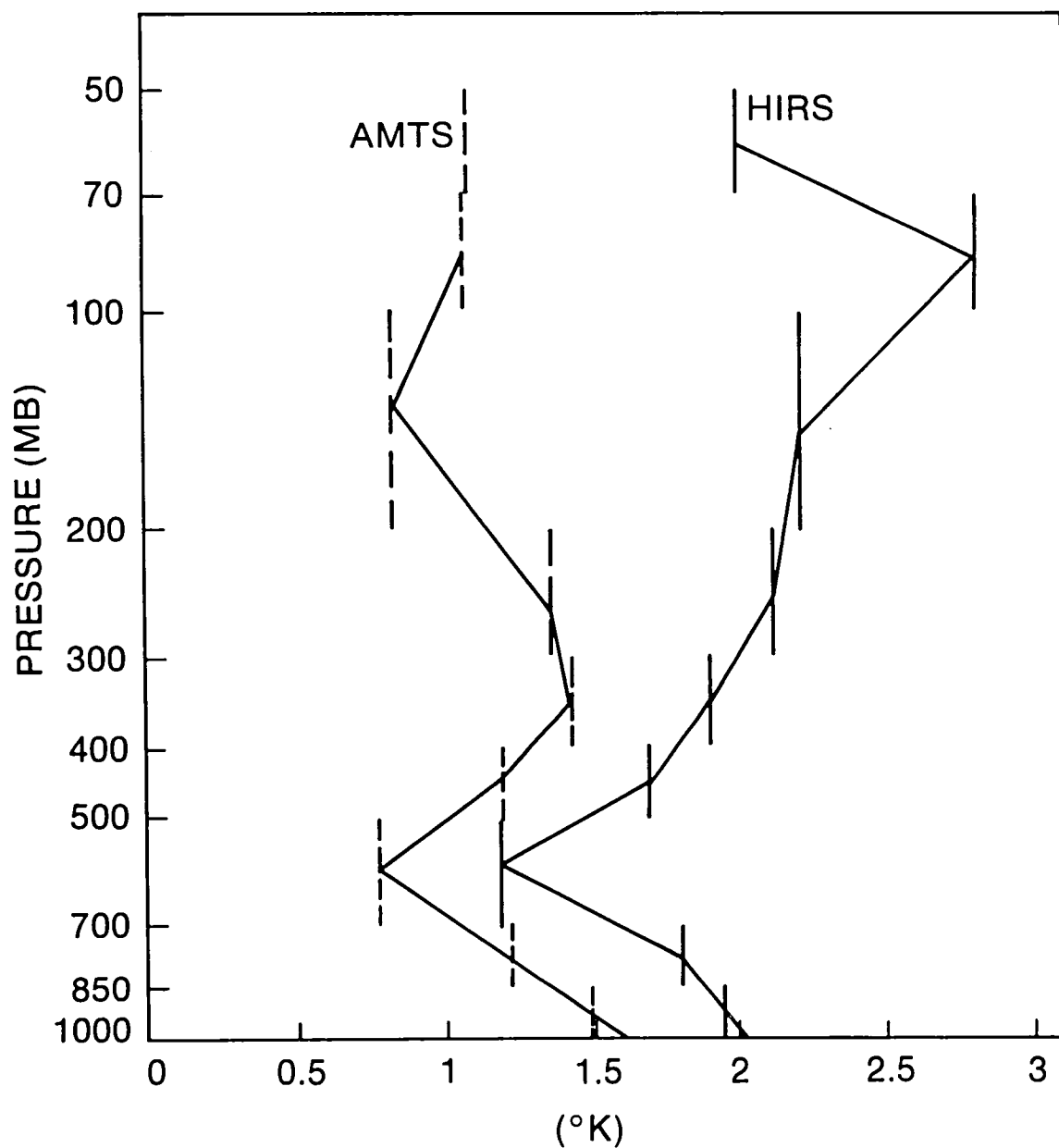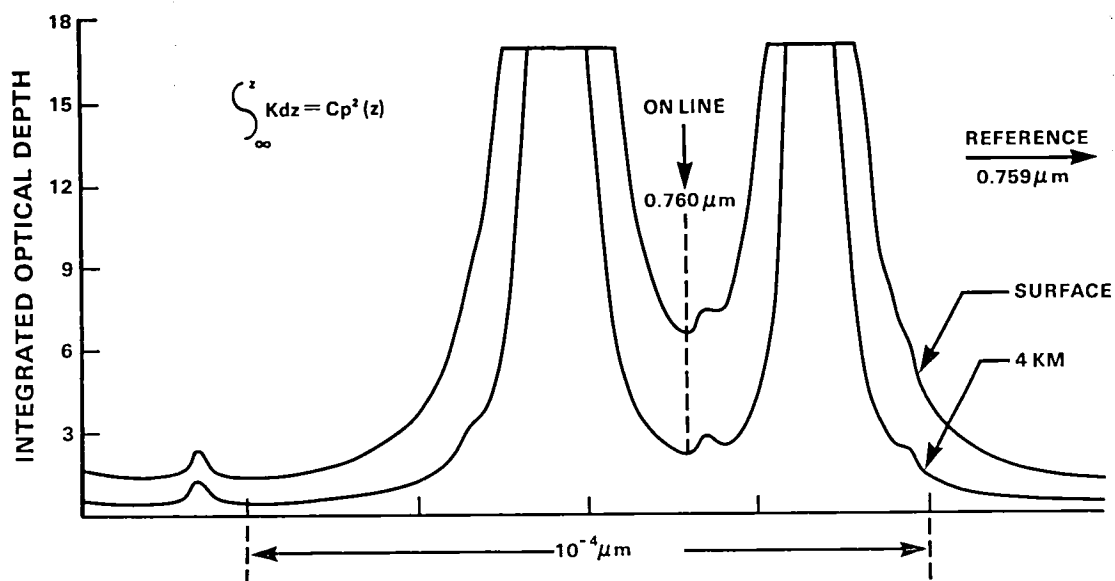# (800 GLOBAL SOUNDINGS)

Figure 9. Simulated RMS temperature errors of the AMTS and HIRS passive temperature sounders as a function of height. Dashed (AMTS) and solid (HIRS) vertical bars indicate layer over which mean layer temperature obtained.

(A)

O₂ EXTINCTION FOR A TWO WAY VERTICAL ATMOSPHERIC PATH

$$\int_{\infty}^{z} K\,dz = Cp^2(z)$$

ON LINE

0.760 μm

REFERENCE
0.759 μm

SURFACE

4 KM

$10^{-4} \mu m$

(B)

TEMPERATURE AND WATER VAPOR PROFILING

ABSORBTION COEFFICIENT

T = 295°K

T = 260°K

λ (REF)

TEMPERATURE $K_L = cT^{-3/2} e^{-E/kT}$ 0.768 μm

WATER VAPOR $K_L = cq$ ($\lambda = 0.724$)

$10^{-4} \mu m$
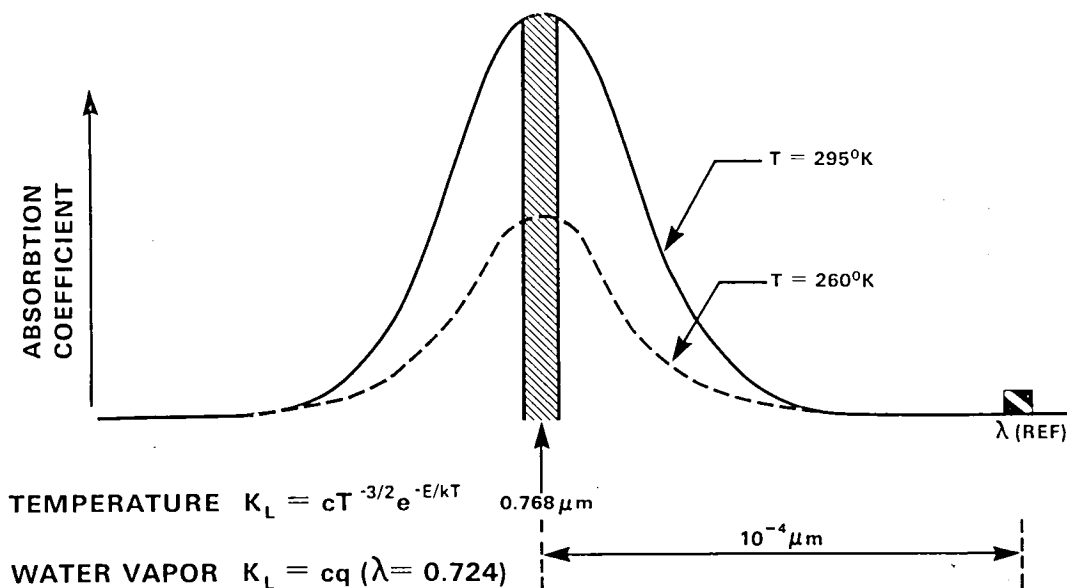
Figure 10. Schematic diagrams illustrating the concepts for lidar measurements of pressure (a) and tempera-
ture (b). Water vapor measurements are analogous to those for temperature. See text.
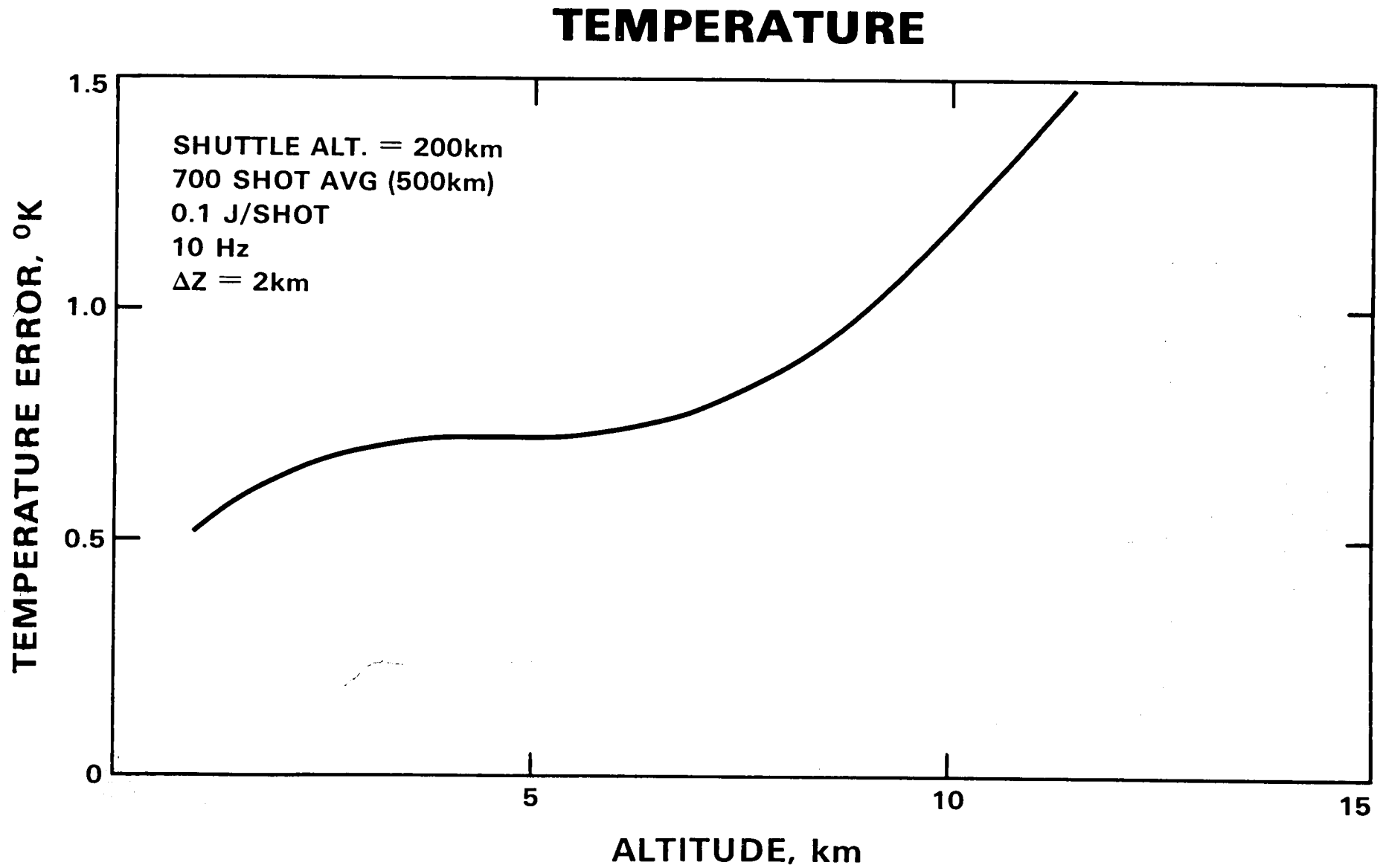
TEMPERATURE

Figure 11. Theoretical accuracy of the DIAL lider temperature profile measurement technique from a spacecraft at 200km altitude. Lidar characteristics as given in Table 3. (After Korb and Weng, 1979b.)
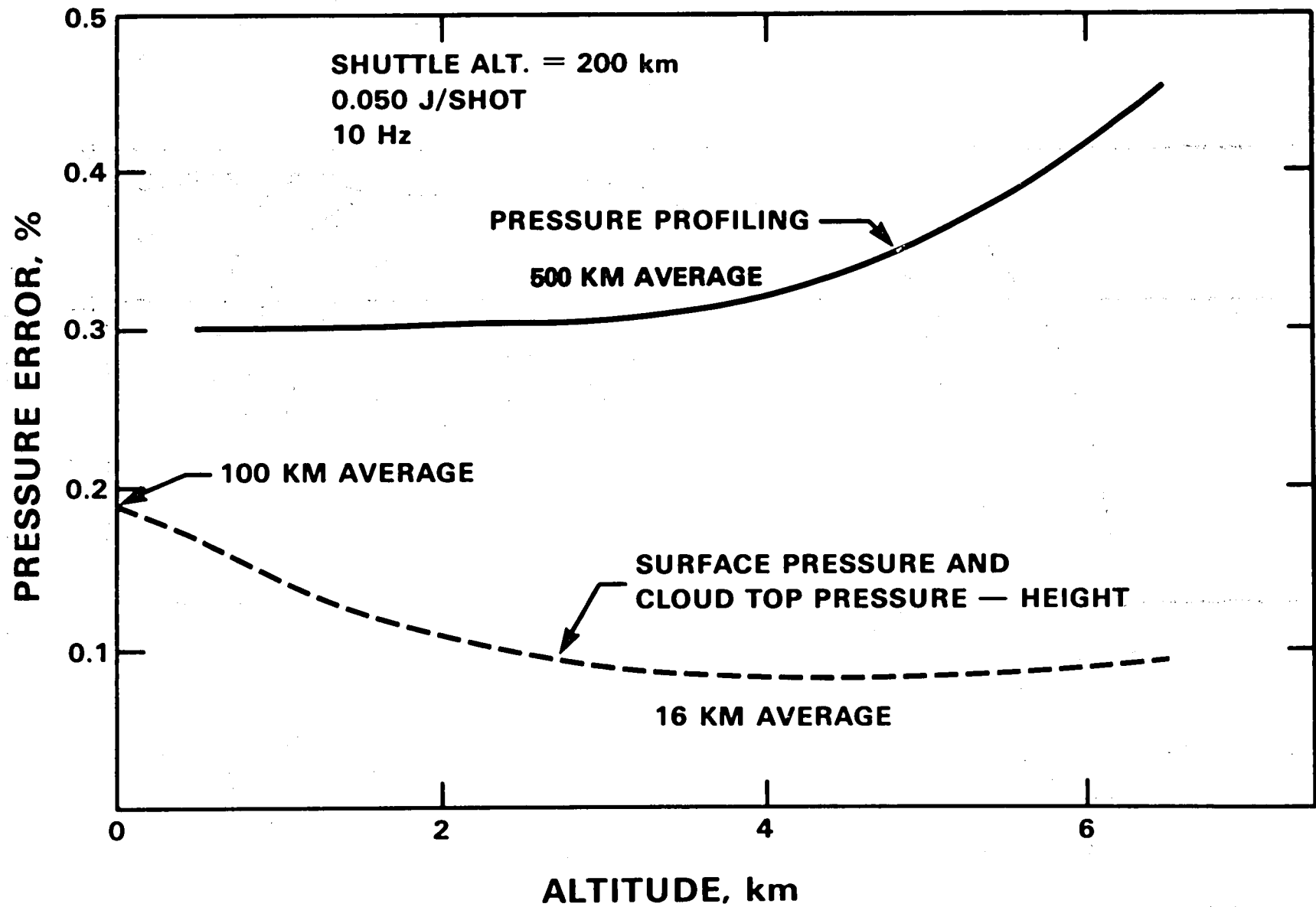
PRESSURE

Figure 12. Dashed curve—Theoretical accuracy of the lidar techniques to measure both surface and cloud top pressure from a spacecraft at 200km altitude. Solid curve—same for the method to measure pressure profiles. Lidar characteristics as given in Table 3. (After Korb et al., 1979a.)
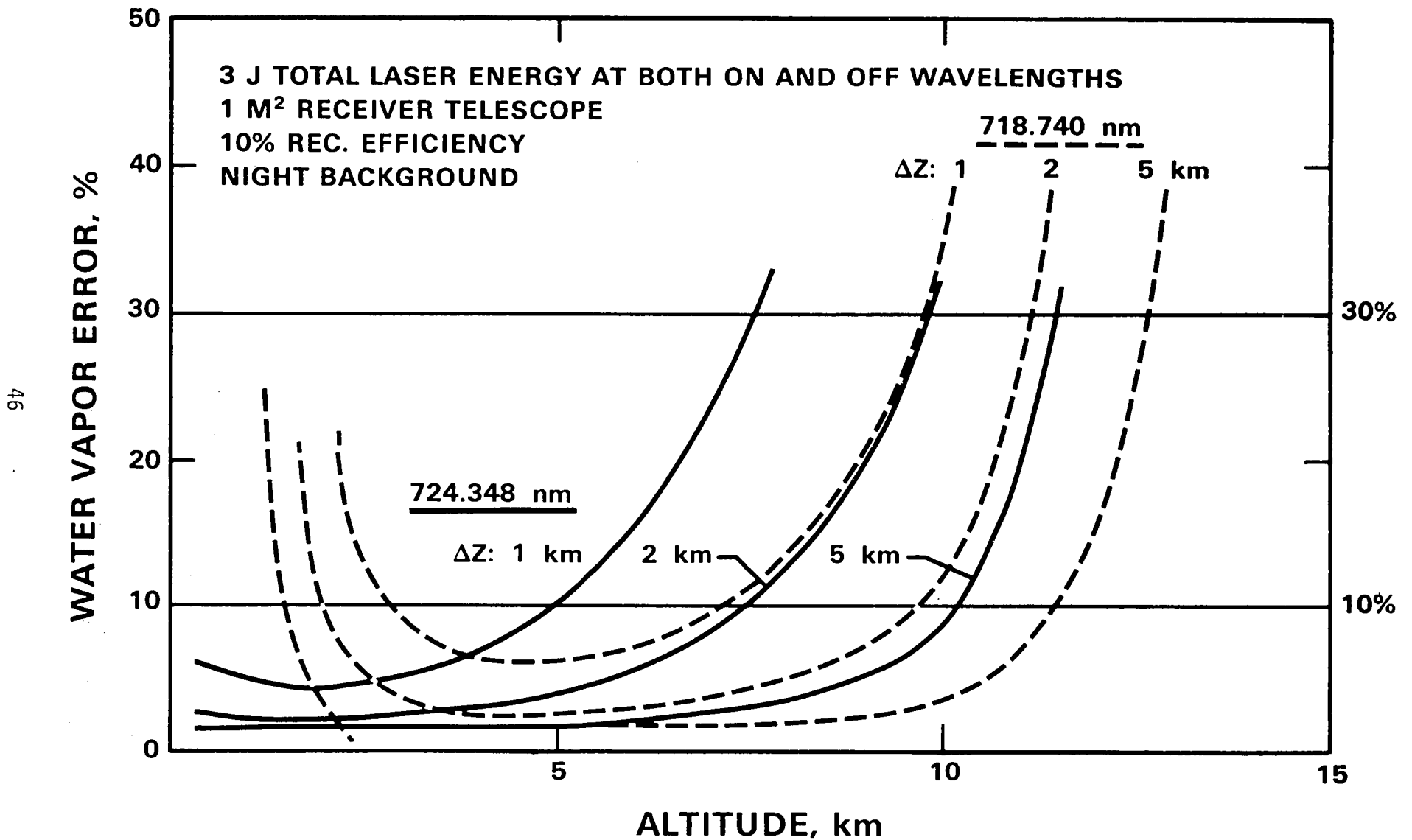
WATER VAPOR

Figure 13. Theoretical accuracy for the lidar techniques to measure water vapor from a spacecraft at 200km altitude. Lidar characteristics as given in Table 3. (After Wilderson and Schwemmer, 1979.)
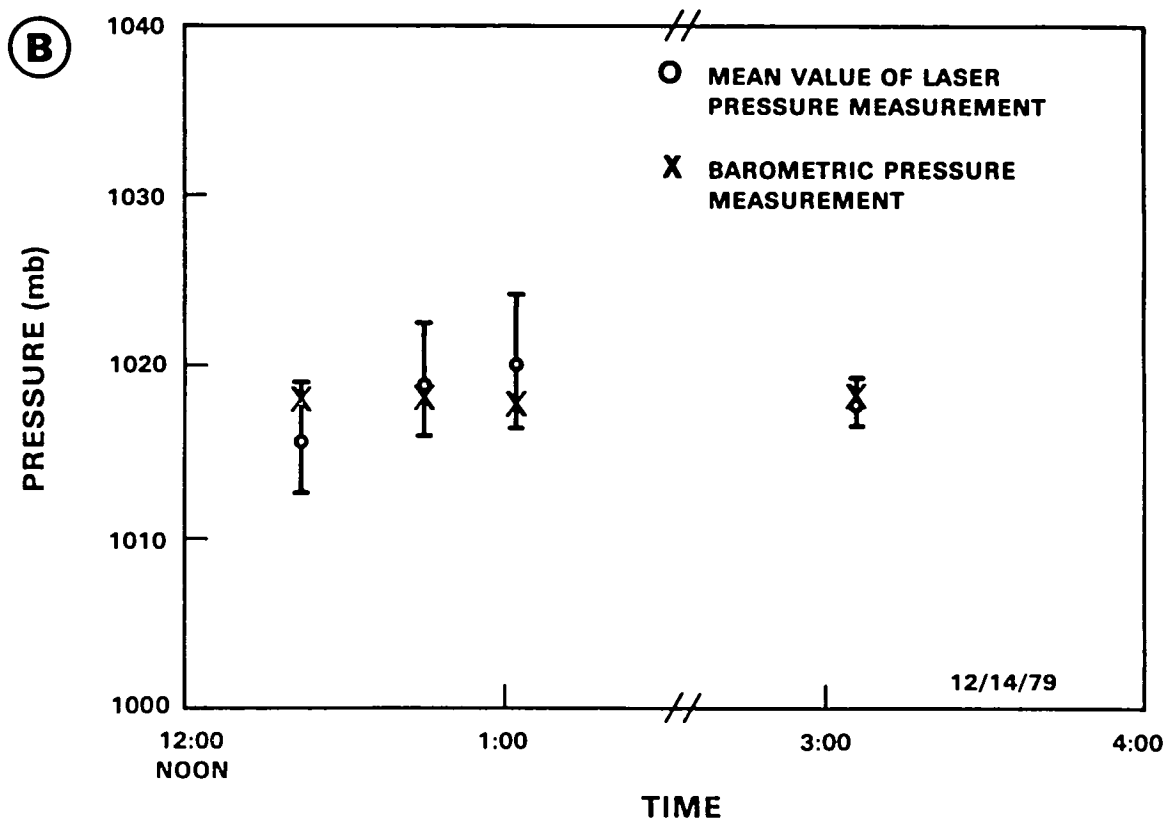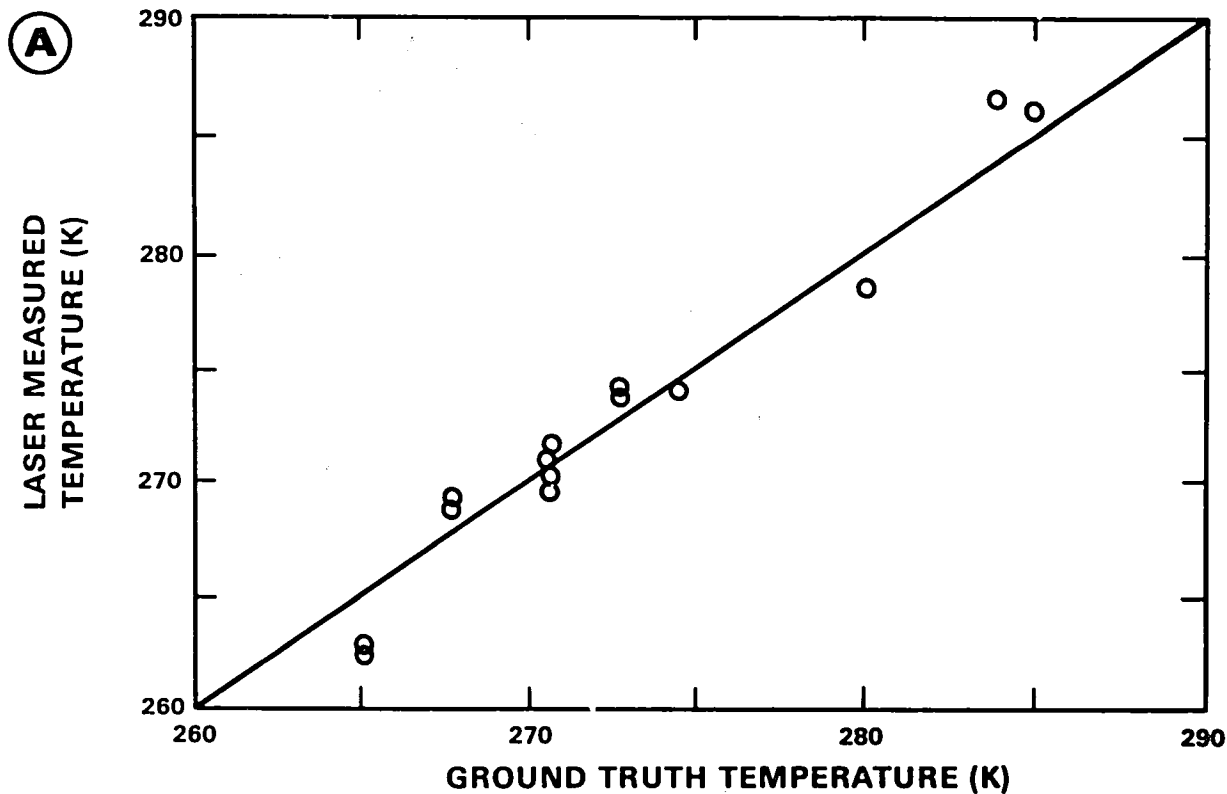
Figure 14. (a) Comparison of CW laser measurements of mean temperature along a 2km round trip path to conventional temperature measurements at a single point. See text. (After Kalshoven, et al., 1980.) (b) Measurements of surface pressure using a CW version of the lidar pressure technique along a 2km round trip path. Error bars indicate one standard deviation uncertainty in laser pressure measurements. (After Korb, 1980.)

47

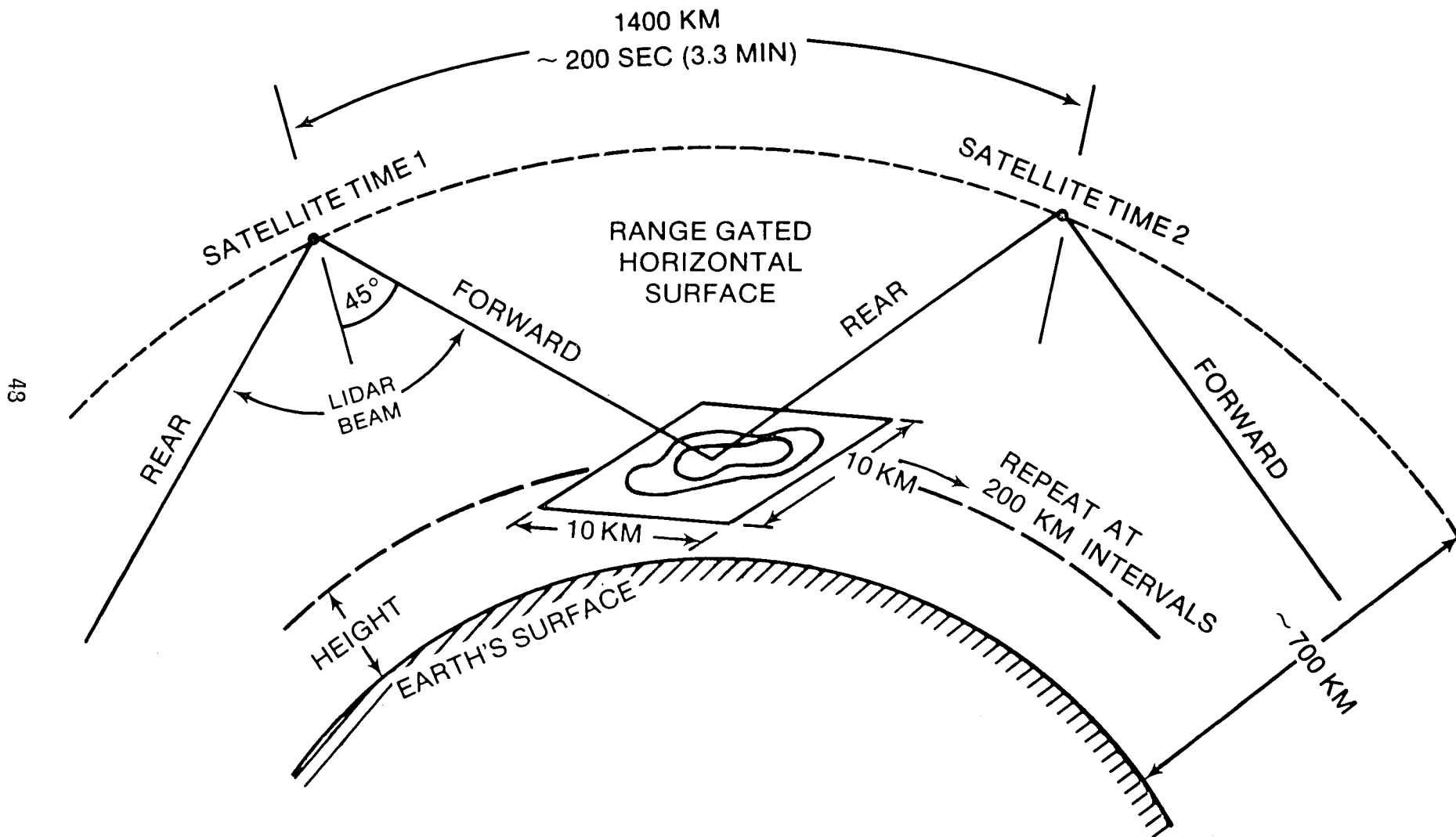# WIND MEASUREMENT BY AEROSOL PATTERN DISPLACEMENT

Figure 15. Conceptual space lidar wind system using aerosol pattern displacement between successive forward and rearward views of same area at constant height. Area scans are repeated at about 200km intervals along orbit. Geometry and timing are nominal, for illustrative purposes only. See text.

BIBLIOGRAPHIC DATA SHEET

1. Report No. TM82006	2. Government Accession No.	3. Recipient's Catalog No.
4. Title and Subtitle WEATHER AND CLIMATE NEEDS FOR LIDAR OBSERVATIONS FROM SPACE AND CONCEPTS FOR THEIR REALIZATION		5. Report Date June 1980
		6. Performing Organization Code
7. Author(s) David Atlas and C. Laurence Korb		8. Performing Organization Report No.
9. Performing Organization Name and Address NASA/Goddard Space Flight Center Greenbelt, Maryland		10. Work Unit No.
		11. Contract or Grant No.
12. Sponsoring Agency Name and Address		13. Type of Report and Period Covered Technical Memorandum
		14. Sponsoring Agency Code

15. Supplementary Notes

16. Abstract

    The spectrum of weather and climate needs for Lidar observations from space is discussed. This paper focuses mainly on the requirements for winds, temperature, moisture, and pressure. Special emphasis is given to the needs for wind observations and it is shown that winds are required to realistically depict all atmospheric scales in the tropics and the smaller scales at higher latitudes, where both temperature and wind profiles are necessary. The need for means to estimate air–sea exchanges of sensible and latent heat also is noted. A concept for achieving this through a combination of Lidar cloud top heights and IR cloud top temperatures of cloud streets formed during cold air outbreaks over the warmer ocean is outlined. Recent theoretical feasibility studies concerning the profiling of temperature, pressure, and humidity by differential absorption Lidar (DIAL) from space and expected accuracies are reviewed. Initial ground based trials provide support for these approaches and also indicate their direct applicability to path-average temperature measurements near the surface. An alternative approach to Doppler Lidar wind measurements also is presented. The concept involves the measurement of the displacement of the aerosol backscatter pattern, at constant height, between two successive scans of the same area, one ahead of the spacecraft and the other behind it, a few minutes later. Finally, an integrated space Lidar system capable of measuring temperature, pressure, humidity, and winds which combines the DIAL methods with the aerosol pattern displacement concept is described briefly.

17. Key Words (Selected by Author(s)) Weather, Climate, Remote Sensing, Lidar Observations, Satellite Observations	18. Distribution Statement		
19. Security Classif. (of this report) Unclassified	20. Security Classif. (of this page) Unclassified	21. No. of Pages	22. Price*